LA-UR- 98-4173

REPORT DOCUMENT PAGE

Report Date: September, 1998

Report Type and Dates Covered In Final Report: June 1, 1995 - September 30, 1998

Title and Subtitle: Measurements of the Ultraviolet Fluorescence Cross Sections and Spectra of *Bacillus anthracis* Simulants

Author: John R. Stephens

Performing Organization: Chemical Science and Technology Division, Los Alamos National Laboratory, P. O. Box 1663, Los Alamos, NM 87545

Performing Organization Report Number:

Sponsoring/Monitoring Agency Names and Addresses:

CDR, USA, CBDCOM, ERDEC
Attn: AMSCB-RRB-M / Rick Lusas
Building: E3330, Room 161
APG-EA, Maryland 21010-5423

Sponsoring/Monitoring Agency Report Number

Distribution/Availability Statement

Distribution Code

Abstract

Measurements of the ultraviolet autofluorescence spectra and absolute cross sections of the *Bacillus anthracis* (Ba) simulants *Bacillus globigii* (Bg), *Bacillus megaterium* (Bm), *Bacillus subtilis* (Bs), and *Bacillus cereus* (Bc) were measured. Fluorescence spectra and cross sections of pine pollen (Pina echinata) were measured for comparison. Both dried vegetative cells and spores separated from the sporulated vegetative material were studied. The spectra were obtained by suspending a small number (< 10) of particles in air in our Single Particle Spectroscopy Apparatus (SPSA), illuminating the particles with light from a spectrally filtered arc lamp, and measuring the fluorescence spectra of the particles. The illumination was 280 nm (20 nm FWHM) and the fluorescence spectra was measured between 300 and 450 nm. The fluorescence cross section of vegetative Bg peaks at 320 nm with a maximum cross section of 5×10^{-14} cm^2/sr-nm-particle while the Bg spore fluorescence peaks at 310 nm with peak fluorescence of 8×10^{-15} cm^2/sr-nm-particle. Pine pollen particles showed a higher fluorescence peaking at 355 nm with a cross section of 1.7×10^{-13} cm^2/sr-nm-particle. Integrated cross sections ranged from 3.0×10^{-13} for the Bg spores through 2.25×10^{-12} (cm^2/sr-particle) for the vegetative cells.

Subject terms: fluorescence, simulants, bacteria, cross sections, Bacillus subtilis, Bacillus globigii, Bacillus anthracis, Bacillus megaterium

Number of Pages:

Security Classification: UNCLASSIFIED

DISCLAIMER

Measurements of the Ultraviolet Fluorescence Cross Sections and Spectra of *Bacillus anthracis* Simulants

by

John R. Stephens
Chemical Science and Technology Division
Los Alamos National Laboratory
Los Alamos, NM 87545

for

US Army - Chemical and Biological Defense Command (CBDCOM)
Aberdeen Proving Ground, MD 21010-5423

September, 1998

Contract Number
W-7405-ENG-36

TABLE OF CONTENTS

LIST OF FIGURES

25 Fluorescence cross sections of *B. globigii* spores and vegetative cells

26 Fluorescence cross sections of *B. globigii* and *B. megaterium* cells

27 Fluorescence cross sections of *B. globigii* cells and pine pollen particles

INTRODUCTION

Fluorescence cross section measurements of biological agents and simulants are needed for the development of both point sensors and standoff detection techniques that use ultraviolet (UV) autofluorescence for detection and identification of biological agents. UV-based point sensors and light detection and ranging (LIDAR) techniques have the potential to detect biological aerosols thereby providing early warning of a biological attack. UV fluorescence can also be used to determine areas of contamination after an attack and to assist in decontamination efforts.

The work reported here is part of a continuing program by the Army's Chemical and Biological Defense Command (CBDCOM) to characterize the ultraviolet fluorescence properties of biological agents. *Bacillus anthracis* (Ba) is a major biological threat agent that is most effectively dispersed as an aerosol of vegetative cells or spores. Biological agent simulants, including *Bacillus subtilis var. Niger sp. globigii* (Bg), *Bacillus megaterium* (Bm), *Bacillus subtilis* (Bs), and *Bacillus cereus* (Bc), included in this report, are closely related to Ba. The Army does, however, maintain facilities for working with Ba.

Our studies were aimed at addressing the following questions regarding the ultraviolet properties of biological agent simulants:

Can vegetative material be distinguished from spores?

Do agent simulants show different spectra when measured in liquid suspension, as dry material, and as suspended particles?

Can biological agent simulants be distinguished from naturally occurring aerosols by their ultraviolet fluorescence?

What are the absolute fluorescent cross sections of Ba simulants?

Recent measurements of agent simulant fluorescence include work by Bronk and Reinisch (1993) who measured fluorescence spectra, including *Bacillus megaterium* and *B. subtilis,* in liquid. Fluorescence cross sections of aerosolized *Bacillus subtilis* have been measured by Faris et al. (1992) in a flowing aerosol stream. Christesen and Ong (1996) have reported extensive measurements of Ba simulants, irradiation-killed Ba, and naturally occurring pollens, etc. suspended in water.

Our measurements are performed on a cloud of particles suspended in an electrodynamic particle trap (EPT) which is capable of suspending single or multiple particles for spectral analysis. A general review of monitoring chemical reactions on single particles is given by Davis et al. (1990). Work by our laboratory on UV fluorescence of agent simulants in liquid suspensions and as bulk powders (Stephens and Rubel, 1996) and of several suspended Bacilli (Stephens, 1996a and b) have been previously reported.

Reported here are ultraviolet fluorescence measurements of Bg, Bm, Bs, and Bc particles suspended in an EPT. The aerosols were illuminated with 280 nm light and the absolute fluorescence spectrum measured in the range of 300 - 450 nm. Spectra of naturally occurring aerosols, including pine pollen (Pina echinata), are also reported.

EXPERIMENTAL

Single Particle Balance Background

The electrodynamic balance or quadrupole trap is an outgrowth of the Millikan oil drop experiment and the electric mass filter of Paul and Raether (1955). Paul and Dehmelt shared the 1989 Nobel Prize in Physics for their work on atomic spectroscopy with the electrodynamic balance. The electrodynamic balance suspends a liquid or solid particle using a combination of AC and DC electric fields that position the particle in the center of the trap and suspend it against the force of gravity. The bihyperboloidal electrode structure we use in our system was introduced by Wuerker et al. (1959).

Single particle traps have been used extensively to perform spectroscopic measurements on suspended particles as outlined in a review by Davis et al. (1990). EPTs have been used to perform Raman spectroscopy (Fung and Tang, 1989), Fourier transform infrared spectroscopy (Grader and Arnold, 1987), and fluorescence analysis from single suspended aerosols (Arnold and Folan, 1986). The extreme sensitivity of fluorescence measurements was demonstrated by Whitten et al. (1991) who demonstrated single molecule detection in suspended particles.

At the beginning of this project the issue was raised that charges on the suspended particles or voltages within the trap would influence the measured fluorescence cross section. Taflin, Ward, and Davis (1989) have explicitly studied the effect of charge on a suspended particle in an electrodynamic trap using optical resonance techniques. They showed that a change in charge of several orders of magnitude had no effect on the optical or physical properties of the suspended particle. Taflin and Davis (1990) also demonstrated that charge has no effect on chemical reactions that occur on a suspended particle. Fourier transform infrared spectroscopy has also been performed on single particles (Grader and Arnold, 1987) and the spectra of the particles were shown to be the same as the bulk solution.

For spherical particles light scattering measurements in a EPT can determine the index of refraction to 5 parts in 10^4 and size to within about 10 Ångstroms (Davis et al., 1990). Optical scattering measurements of single suspended particles are the preferred technique to determine index of refraction of National Institute for Standards and Technology (NIST) standard spheres (Mulholland et al. 1985). These measurements show that a suspended particle has the same optical properties as the bulk material indicating that the optical properties of a suspended particle is not influenced by either the charges on the particle or the voltages applied to the trap.

Experimental Apparatus

In our EPT apparatus, the single particle spectroscopy apparatus (SPSA), the particle size and also the fluorescence spectra and cross section can be measured. Fluorescence is measured using a calibrated light source, collection optics, and detector. Particle size is determined by measuring the angular dependence of light scattering in the forward scattering direction (35 - 55 degrees scattering angle). For nearly spherical particles the angular separation of the peaks in scattered light intensity may be related to the particle size (Gouesbet and Grehan, Eds., 1991).

A schematic of the SPSA is shown in Figure 1. Light from a 100 watt Mercury Hg) arc lamp is collected using quartz lenses and reflected through three reflection dichroic filters which have a transmission cut at 340 nm. The light is focused onto a tapered quartz optical fiber that is F number matched to the light source. The excitation light is transmitted to an optical coupler, again F number matched to the fiber optic, passes through a transmission filter with a 50% transmission cut at 300 nm, through another dichroic reflection filter and is then focused to the center of the particle trap. The measured output

of the arc, before and after filtering, is shown in Figure 2. As shown in the Figure the output of the lamp is reduced at least 6 orders of magnitude above 300 nm wavelength while the output at the excitation wavelength (270 - 290 nm) is reduced less than a factor of 10. This highly pure emission is necessary to measure the autofluorescence of the bacteria which have very low cross sections relative to their physical cross section. If the excitation light intensity is not reduced to below the fluorescence level the spectrometer/detector would see only excitation scattered light from the particle.

The total excitation light focused into the particle trap is typically 50-60 μW in a 280 μm diameter spot. A secondary peak in the excitation spectrum, centered at 250 nm, has an integrated emission a factor of 10 less than the principal excitation peak. Calibration of the SPSA is discussed in detail below.

Fluorescent light from the particle may be collected either at 90 degrees or 180 degrees from the excitation light direction. For the 180 degrees collection the fluorescence light is collected after passing through the dichroic filter used to direct the excitation light into the trap. The fluorescence light is filtered by two high pass optical filters with a 50% cut-on wavelength of 300 nm. In addition the light passes through a colored glass filter that blocks the Helium Neon (HeNe) laser light (628 nm) scattered from the particle. The fluorescence light is then transmitted via a tapered fiber optic that is F number matched to the collection optics and the spectrometer.

For these experiments all of the fluorescence spectra were obtained with the excitation light 90 degrees from the fluorescence collection optics. This configuration is different than the geometry in which fluorescence intensity is measured in the field using LIDAR. In the field studies, the backscatter (180 degrees) fluorescence is measured because the 90 degree fluorescence is not available since the measurements are made in a standoff configuration. The difference in geometry of the excitation and collection optics produces a large difference in background light. The 180 degree collection angle has a much higher background level of scattered (non-fluorescent) light than the 90 degree configuration. This is illustrated in Figure 3 which shows measured background levels of scattered light at 90 and 180 degrees collection optics. The background at 180 degrees collection is at least 25 times that at 90 degrees between 300 and 450 nm. For this reason all of the spectra shown in this report were taken in the 90 degrees collection angle configuration.

The spectrometer (Chromex ChromSpec 250is Imaging Spectrograph) is a single grating instrument that is optimized for imaging. For these measurements a 300 g/mm grating and 1000 μm wide slits were used to match the diameter of the optical fiber (600 μm).

The fluorescence light was focused onto a liquid nitrogen-cooled charged coupled detector (CCD) with 1024 elements over a 600 μm x 25 mm area (Photometrics SDS 900 cooled CCD system). The detector was overcoated with a fluorescence coating to provide a high quantum efficiency in the spectral range of 200 - 600 nm. The combination of the spectrometer and detector allowed the spectral range of 290-450 nm to be measured at a single spectrometer setting. No scanning of the spectrometer was required. The spectral resolution was 0.3 nm/pixel. The CCD has a noise figure of less than 0.01 photons/second/pixel. To further reduce detector noise we hardware binned the CCD during readout. Detector dark current levels, subtracted from the spectral signal, were taken from the upper portion of the CCD that was not illuminated by the fluorescence spectrum. Figure 4 shows a typical image of the fluorescence on the detector. The background region is above the illuminated area on the detector. To obtain spectra with high signal to noise, the spectra were integrated on the detector between 1 and 100 seconds. After the integration time a spectrum was read out and transferred to the computer for analysis. To obtain a spectrum pixels were accumulated vertically for the signal and background regions and the difference taken to produce the final spectrum. Calibration curves of the sensitivity of collection optics, spectrometer, and CCD were applied to the

collected spectrum to produce a calibrated spectrum from which the cross sections were derived.

A photograph of the SPSA is shown in Figure 5. A detailed schematic of the particle trap and associated equipment is shown in Figure 6. Here, in addition to the fluorescence excitation and collection optics, are shown the Helium Neon (HeNe) laser path and video camera, used to image the particles, and the angular scattered light detector, used for particle sizing.

The video system consists of a 5 mW HeNe laser that passes through the chamber at 45 degrees from the collection optics. The video camera, which is attached to an optical microscope, images the particles within the ultraviolet excitation volume of the trap. The magnification of the optical system can be changed from 4 to 40. The video system is used for alignment of the excitation and fluorescence collection optics and to count the number of particles within the excitation volume during the exposure time of the CCD detector.

After injection of particles into the trap and stabilization of a single particle or cloud of particles the video image is recorded during the fluorescence collection period. The images are then digitized from the videotape and the number of particles counted. The number of particles within the collection volume is used to normalize the collected spectrum to determine the absolute cross section per particle.

The angular dependence of light scattered by the HeNe laser is used to determine sizes of individual particles in the trap. The angular scattered light detector, a silicon detector array (Princeton Applied Research Detector Model 1412), has 1024 detectors which cover the angles between 35 and 55 degrees scattering angle. For nearly spherical particles the angular spacing between the scattering maxima and minima are a monotone function of the particle size when the index of refraction is known. A comparison between the calculated and measured scattering profiles of bacterial particles is shown in Figure 7. Here the calculated scattering profiles are normalized to 1 in the forward (angle=0) scattering direction. Optical constants of *Bacillus subtilis* (n=1.52, k=0.0166) from the literature (Arakawa et al., 1995) were used in the calculation. The optical constants of *B. megaterium* are expected to be very similar. The calculated data are shown for particles between 0.5 and 4.0 microns in radius. The angular difference between the maxima range from 30 degrees for the 0.5 μm particles to about 5 degrees for the 4.0 μm particle. Shown also in the Figure is our measured scattering profile for a single Bm particle. The peaks are not as distinct as the calculated scattering peaks, as expected, since the particles are not highly spherical. The spectrum covers only a few scattering peaks, but the difference in scattering angle shows the particle to be between 2 and 4 microns radius. Because of the difficulty in isolating a single particle during fluorescent measurements, simultaneous measurements of fluorescence and size were not obtained in this study.

Calibration

A key component in measuring absolute fluorescence cross sections is the spectral irradiance calibration of the excitation and fluorescence optics, spectrometer, and CCD detector. To calibrate the fluorescence from small particles the calibration system needs to simulate the emission of small particles, both in terms of the irradiance and particle geometry. This essentially means creating a virtual particle with known radiance that can be used to calibrate the fluorescence optics.

A schematic of the calibration system is shown in Figure 8. An artificial particle is created by illuminating an optical integrating sphere (Labsphere LM-4000 Radiometer) using a deuterium (D_2) or tungsten standard lamp that are traceable to the National Institute of Standards and Technology (NIST). A calibrated 100 μm pinhole on the side of the sphere forms a virtual particle with known radiance (μW/sr-nm). The fluorescence optics, including the entrance filters, lenses, and fiber optics, are plugged into a jig which then carries the light to the spectrometer and CCD detector. The geometry of the calibration jig is the same as the geometry of the particle trap and the collection optics are unplugged from

the calibration setup and plugged into the particle trap after calibration. The calibration calculations are given in Equations 1 and 2. The lamps illuminate the integrating sphere through a hole of known size thereby producing a know irradiance ($\mu W/cm^2$-nm) into the sphere. This quantity is known for the standard lamps. Knowing the surface area of the sphere, sphere reflectance, and pinhole area allows the radiance (μW/sr-nm) from the pinhole to be calculated.

Fluorescence Spectrum:

$$C_f(l)\ (cm^2/sr\text{-}nm) = [(I_s/I_{std})*L_e(l)]/F_{excit} \qquad (1)$$

with:

I_s/I_{std} the ratio of detector counts/s of the Bacillus fluorescence to counts from a standard lamp illuminating the integrating sphere

$L_e(l)$ is the radiance spectrum of the standard lamp exiting a pinhole in the integrating sphere (μW/sr-nm)

F_{excit} is the total irradiance of the excitation source ($\mu W/cm^2$)

Calibration:

$$L_e(l)\ (\mu W/sr\text{-}nm) = r\,F_i(l)\,A_e/p\,A_s\,(1\text{-}r(1\text{-}f_j)) \qquad (2)$$

with:

p the sphere wall reflectance ($0 < r < 1$)

$F_i(l)$ the incident flux through the sphere entrance (μW/nm)

A_s the surface area of the sphere (cm^2)

f_j the ratio of port areas to sphere surface area

A_e the area of the exit port (100 μm pinhole)

To calculate the fluorescence cross section of the particle one needs to know the irradiance of the source ($\mu W/cm^2$-nm) on the particle. With the calibration of the fluorescence optics discussed above, the cross section can be calculated. To measure the spectrum of the excitation source the excitation optics and fiber are unplugged from the trap and plugged into the integrating sphere. The spectrum is measured using the fluorescence optics attached to the integrating sphere but viewing the sphere without the pinhole. The sphere is them illuminated with the standard lamps to calibrate the excitation spectrum. This procedure gives the excitation spectrum. A typical spectrum is shown in Figure 9. The spectrum peaks at 280 and 287 nm with a FWHM of 20 nm. The integrated excitation intensity is 50-60 μW.

To obtain the excitation irradiance onto the particle the excitation and fluorescence spot size (cm^2) at the center of the trap must be known. The excitation spot is formed as a real image of the end of the excitation fiber optic. The focal length is adjusted to ensure that the focus is at the center of the particle trap. The focus is adjusted in a special jig in which the excitation optics are focused onto a scintillation plate at the required distance. The

image is recorded on video tape and used to derive the irradiance ($\mu W/cm^2$ -nm) onto the particles in the trap. An irradiance spot, measured using the video system, shown in Figure 10, is about 300 μm in diameter. The focus of the fluorescence optics is also fixed in a similar manner using the same optical jig. A typical "spot" or area from where the fluorescence is collected, is shown in Figure 11. The fluorescence spot is smaller than the excitation spot to minimize intensity variations across the active volume in the trap.

After the excitation and fluorescence fiber optics have been focused to correspond to the position of the particle in the center of the trap the optics are unplugged from the calibration jig and attached to the particle trap. A scintillation fiber is positioned to the center of the trap and the lateral positions of the excitation and fluorescence optics are adjusted so that their volumes overlap in the trap center. The typical position of the excitation and fluorescence volumes are shown in Figures 12 and 13 where light through the optics is striking the 300 μm scintillation fiber. The images are obtained by the video system that is used to image the particles in the optical volume of the trap. The optical volume is recorded on video tape to determine the number of particles within the volume to determine particle cross sections. The NeHe laser, used to illuminate the particles, is also aligned to correspond to the optical volume, an example of which is shown in Figure 14.

The uncertainty in the calibration measurements is determined by the stability of the standard lamps (~ 2%), the degree to which all of the calibration routines can be reproduced, including spot size and alignment, and the stability of the spectrometer and CCD detector. The variation in the calibration using the D_2 and tungsten lamps over a 5 month period are shown in Figure 15. The limit curves are +- 10% which bracket the range of the calibrations. The two lamps show good correlation above about 325 nm, but differ increasingly below 325 nm. Because the tungsten lamp output is rapidly falling below 350 nm and the D_2 lamp shows increasing output in this region the calibration curves were spliced at about 350 nm to form a single calibration curve. Uncertainties for the absolute lamp calibrations exceeded 15% below 325 nm.

We were unable to measure the total uncertainties of the fluorescence cross sections because this requires that a standard particle of known size and fluorescence cross section be used. Such a particle is unavailable. Total uncertainties include all of the variations in the calibration lamps, as discussed above, as well as alignments in the calibration jib, focusing and alignment of the excitation and fluorescence optics in the particle trap, as well as variation of efficiencies for the excitation and collection optics. A formal error analysis has not been done but an estimate of the overall uncertainties is a factor of 5 for the absolute cross sections. For the shape of the fluorescence spectrum, about a +- 50% uncertainty is reasonable.

Sample Preparation and Particle Injection

Bacterial strains were obtained from the American Type Culture Collection (ATCC) or from Dugway Proving Grounds (DPG) that is part of the Army's Chemical and Biological Defense Command (CBDCOM). In the latter case the samples (*Bacillus subtilis var. Niger sp. globigii* (Bg)) were characterized as received and also re-grown to ensure sample purity. The samples from the ATCC were Type Strains from the *Bacillus* genera (wildtype strains) listed below:

a) *Bacillus globigii* - ATCC # 9372

b) *Bacillus cereus* - ATCC # 7064

c) *Bacillus megaterium* - ATCC # 14581

d) *Bacillus subtilis* - ATCC # 6051

Samples were grown in nutrient broth. For the sporulated samples the pH was changed to induce sporulation. Spore separation was carried out using Metrazoic acid to produce a density gradient during centrifugation. Both sporulated and unsporulated samples were washed repeatedly with distilled water and lyophilized for injection into the SPSA. Bm, Bc, and Bs samples with low sporulation efficiency, high-efficiency sporulated Bg, spore-separated Bg samples, and unsporulated (vegetative) Bg samples measured.

Bacterial samples were counterstained and examined using optical microscopy to ensure sample purity. Figure 16 shows an optical micrograph of the Bg as received from DPG. In the micrograph the spores appear as blue green spheres and other materials appear pink. The DPG material was grown, sporulated, and then ball milled to reduce the particle size for effective dispersion. No spore separation was carried out during preparation of the DPG samples. The material in the micrograph may contain milling materials as well as spores and degraded vegetative material. To avoid spurious ultraviolet fluorescence we regrew the material from DPG, using the same procedure used for our other samples, before measuring its fluorescence.

Optical micrographs of two samples of *B. cereus* and *B. megaterium*, grown at Los Alamos from ATCC samples, are shown in Figure 17. These micrographs were taken using phase contrast microscopy to increase contrast. The bacteria are rod-shaped cells that occur in tangled chains with dimensions about 1 x 10 μm. The *B. megaterium* has a much larger diameter than the *B. cereus*. Note that our bacteria look much different than the DPG samples that have been sporulated and that contain vegetative material that is highly degraded. The complexity of the shape and size of the bacterial clusters make the definition of a single fluorescence cross section problematic. The fluorescence cross section of various clusters will vary by at least an order of magnitude depending on the size of the clusters examined.

To assess the size distribution of bacterial clusters being injected into the SPSA we measured their aerodynamic size distribution. The *Bacilli* from the growth and preparation stages were lyophilized (dried) in a freeze drying apparatus that produced a fluffy dry powder. The powder was transferred to a hand-powered nebulizer similar to a perfume sprayer but for powders. For the measurements particles were injected into the trap as a cloud of dry particles directly from the nebulizer. This procedure produced a large amount of air currents within the trap which carried the particles throughout the trap. After most of the air currents died down a cloud of particles or, in some cases, a single particle was trapped. Multiple particles in the trap are not retained at the center of the trap but assume complex orbits about the trap center because of mutual electrostatic interactions between the charged particles. Typically, about 10 or less particles were trapped within the active volume of the trap and were used for fluorescence measurements. It was very difficult to reduce the number of particles from about 10 to a single particle because the particles have very similar charge. Changing the controlling voltages of the trap tended to retain all or none of the particles with a very slight change in voltage. We are developing a technique for injection and suspension of single particles that are compatible with both the scattering and fluorescence measurements. The dispersion method is distinctly different from that used at field trials at DPG where air-driven agricultural sprayers are used for dispersion. For the size measurements we blew the lyopholized bacteria into a chamber and drew samples into a real-time cascade impactor that separates particles by aerodynamic size into 7 size bins between 0.1 and 10 μm and measures the mass in each bin. The instrument provides a mass size distribution rather than a number density distribution provided by optical aerosol counting instruments. The size distributions before and after spore separation, using the dry injection method, are shown in Figure 18. Before spore separation the sporulated sample has a size distribution with a mass peak near 1 μm with little mass below 1 μm. The nominal single spore size is 1 μm. A substantial fraction of particles are up to and above 10 μm in aerodynamic size. After sporulation the size

distribution is peaked in the 3-5 μm range with very little mass below 1μm and above 7 μm. The resulting particles contain little vegetative material and contain 1 - 50 spores.

RESULTS

Liquid Suspension Measurements

Initial measurements of fluorescence from Los Alamos and DPG bacteria were made using a commercial fluorescence spectrometer (Perkin Elmer Model LS5). These measurements were carried out to answer some of the questions posed at the start of the research effort:

> Do agent simulants show different spectra when measured in liquid suspension, as dry material, and as suspended particles?
>
> Do various *B. anthracis* simulants show different fluorescence spectra?

Fluorescence and excitation spectra were measured on lyopholized bacteria that had low and high sporulation efficiencies as determined by optical microscopy. Spectra were obtained on liquid suspensions with sufficient bacterial concentration to produce spectra of good signal to noise. Cross section measurements were not made. The results are shown in Figure 19. Spectra were obtained on sporulated *B. cereus, B. globigii, B. megaterium, and B. subtilis.* Excitation was centered at 280 nm to match the excitation wavelength of the single particle trap. The fluorescence spectra in the Figure are normalized and offset for illustration. All of the spectra show the same fluorescence peak centered at 320 - 325 nm. The wavelengths below 320 nm show variable intensities in these spectra because of limited spectral selectivity of the single grating instrument which allows some leakage of the water Raman line and excitation light into this wavelength range. We did not observe in these spectra variations in the shape of the spectra versus sporulation efficiency. These results are in agreement with previous work on dry Bg aerosols (Faris et al., 1992) and Bg in water suspension (Ong and Christesen, 1996) shown in Figure 20.

Measurements were also taken of the excitation spectrum of water suspensions of Ba simulants by monitoring a fixed (350 nm) fluorescence wavelength and scanning the excitation wavelength. The results of several Los Alamos grown *Bacilli* and the DPG Bg material (not re-grown at Los Alamos) are shown in Figure 21. The spectra are again offset and normalized for comparison. For all of the Los Alamos grown bacteria, independent of the species, the peak fluorescence emission occurred at an excitation wavelength of 280 nm. All of these samples were sporulated but not spore separated. For the DPG Bg spores however the peak in excitation curve occurs near 290 nm and shows a very different shape. Comparison of the optical micrographs of the DPG material (Figure 16) and the Los Alamos grown bacteria (Figure 17) shows substantial non-spore material present in the DPG sample, which may be degraded vegetative material as well as milling additives. We believe that these materials give rise to the different excitation seen in the Figure. For all subsequent spectral studies the DPG material was re-grown using our standard procedure to ensure extraneous materials in the sample did not contribute to the measured fluorescence.

Demonstration of Single Particle Fluorescence

To demonstrate the validity of measuring the fluorescence from single particles using the SPSA, we measured the fluorescence from a 6 μm latex sphere that had been doped to make them fluorescent (Duke Scientific Series 35 Fluorescent Microspheres). Because the fluorescent dopant concentration is not determined in preparation of the

microspheres, it was not possible to use these spheres for fluorescent cross section calibrations. The peak excitation wavelength was 458 nm with the peak emission spectrum at 512 nm. The excitation optics of the SPSA were modified to isolate the 436 nm Mercury line from the arc lamp. The fluorescence optics were set up to block the 436 nm excitation line and pass the emission band. A photograph of a suspended single fluorescent particle, in the SPSA, is shown in Figure 22. The particle is clearly seen by its fluorescence as the light blue dot in the center of the trap. The fluorescence spectrum, obtained with a ten second exposure, is shown in Figure 23. The demonstration proved our ability to suspend a single particle in the SPSA and to measure its fluorescence but significant work was required to measure the much smaller fluorescence cross section of biological particles. Also, biological particles are much more difficult to suspend than latex spheres because they do not accept or hold charge nearly as well as the latex microspheres.

Comparison of Fluorescence from Liquid Suspensions, Bulk Dry Powders, and Single Particles

We measured the fluorescence spectra of liquid suspensions, bulk dry powder, and single particles of *B. cereus*. For the liquid suspension measurements we used the commercial spectrometer discussed above. The "bulk" powder (lyophilized bacteria) measurements used all of the source and fluorescence components of the SPSA but rather than attaching the excitation and fluorescence fibers and optics to the particle trap we illuminated the lyophilized *B. cereus* powder on fused silica substrates. This arrangement tested the spectral calibration of the system and allowed comparison with spectra obtained using the commercial spectrometer. Single particle measurements were also made for comparison using the optics fitted to the optical trap. The results of these measurements are shown in Figure 24 which compares the normalized and offset spectra of liquid suspension, bulk powder, and single particle spectra of *B. cereus*. In all cases the excitation wavelength was 280 nm. The peak in the fluorescence spectrum for all samples is 320 - 330 nm. The single particle spectrum was quite noisy in this Figure because we were using an early version of the CCD detector that showed substantial detector noise in some regions of the detector. A liquid nitrogen-cooled CCD detector was used in later experiments. The spectra show that there is no difference between spectra of a Ba simulant in liquid suspension, dry powder, and single particle form. Thus, comparison of various laboratory's spectra, taken using various sample preparation techniques, is a valid procedure.

Measurement of Fluorescent Cross Sections from *B. anthracis* Simulant Particles

Spectra and fluorescence cross sections were made on dry (lyophilized) bacteria that were grown without spores (vegetative), cells that were sporulated but without separating the spores from the vegetative cells (sporulated), and on spores separated from the vegetative cells (spores). Spectra were obtained on a small number of particles within the optical volume of the trap and normalized per particle as discussed above. The spectra of *B. globigii* vegetative cells and spores are shown in Figure 25. The vegetative Bg samples show the highest fluorescence cross section with the peak at 320 nm and a maximum cross section of 5×10^{-14} cm^2/sr-nm-particle. The total fluorescence cross section is 2.3×10^{-12} cm^2/sr-particle. In contrast, *B. globigii* spores show a peak fluorescence cross section at 310 nm with peak fluorescence of 8×10^{-15} cm^2/sr-nm-particle. Integrated fluorescence cross section is 3.0×10^{-13} cm^2/sr-particle.

The fluorescence cross sections for both of our Bg samples are higher than the cross sections measured for Bg vegetative cells by Faris et al. (1992) who report a value of 3.5×10^{-15} cm^2/sr-nm-particle for dry aerosols. Our Bg vegetative cells have an order of magnitude larger cross sections than Faris et al. They report Bg wet aerosol cross sections

of 1.6 X 10^{-14} cm^2/sr-nm-particle and liquid suspension cross sections of 4.0 X 10^{-14} cm^2/sr-nm-particle. Our larger cross sections than Faris et al. may be partially due to the higher excitation efficiency at 280 nm relative to the 266 nm excitation used by Faris et al..

A comparison of the fluorescence cross sections for *B. megaterium* and *B. globigii* samples are shown in Figure 26. The Bm particles were sporulated vegetative cells while the Bg particles were unsporulated vegetative samples. The Bm sample shows a peak fluorescence cross section of 2 X 10^{-14} cm^2/sr-nm-particle at 315-320 nm. The Bg vegetative cells have a peak fluorescence of 5 X 10^{-14} at 320 nm. The slight peak shift toward shorter wavelengths for B. megaterium represents the contribution of the spores in the Bm cells relative to the spore-free Bg cells. The cross section of the Bm is a factor of 2.5 less than the Bg cells. Without simultaneous measurement of the particle size and fluorescence cross section it is not possible to determine if the higher cross section of the Bg cells is due to larger size particles or higher fluorescence efficiency.

Our spectra were similar to fluorescence spectra of Bronk and Reinisch (1993) who measured liquid suspensions of *B. cereus, B. subtilis*, and *B. megaterium* using an excitation wavelength of 280 nm. They saw a shift to shorter wavelengths from the vegetative to spore forms which we also observe. Our peak fluorescence cross section for Bg spores is lower than the value (3 X 10^{-14} cm^2/sr-nm-particle) for Bm spores in liquid suspension. It is generally agreed that spores and vegetative cells in solution show higher fluorescence cross sections than as dry suspended particles. The fluorescence spectra for Bm and vegetative Bg reported here are similar to our previous measurements in solution and as bulk powders (Stephens, 1996 a, b).

Measurement of Fluorescence Cross Section of Pine Pollen

To access the potential fluorescence interferences of naturally occurring aerosols with bacterial fluorescence, we measured the fluorescence cross section of pine pollen (*Pina echinata*). The pine pollen was injected into the trap as dry powder, the same method used for the bacteria. The particles were all greater than 10 μm in aerodynamic diameter as measured by the real-time cascade impactor. A fluorescence spectra of the pine pollen, together with the spectra of *B. globigii* vegetative cells, are shown in Figure 27. The spectra are clearly distinguishable with the pine pollen fluorescence peaking at 355 nm, well longward of the B. globigii fluorescence peak at 320 nm. The pine pollen peak fluorescence cross section is 3-4 times greater than the bacteria with strong fluorescence carried out to at least 400 nm. Since the pine pollen particles are larger than the *B. globigii* particles we expect the fluorescence cross section to be larger. At this time we can not determine if the efficiency of fluorescence is greater for the bacteria or the pine pollen because of uncertainties in the size of the particles. Our fluorescence spectrum of the pine pollen is similar to that measured for pine pollen in water suspensions by Christesen (1997).

CONCLUSIONS

Differences in cross section may result in differences in size as well as fluorescence cross section. Measured size distributions (Figure 18) show the that the spore-separated sample are larger than the sporulated sample, but we have not measured the sizes of the individual particles on which the fluorescence measurements were made. We are currently working to develop a single particle injection system that will allow us to make simultaneous measurements of fluorescence cross section and size.

Our fluorescence measurements are similar to other researchers, as noted above, in the shape of the spectral curves, but the absolute cross sections differ up to an order of magnitude between reported studies. The major uncertainty in fluorescence cross section measurements, made by ourselves and others, is the size of the particles on which the

measurements are being made. The SPSA has the potential to suspend single, well characterized, biological particles and measure their absolute fluorescence spectrum and size. This is in contrast to fluorescence measurements on liquid suspensions or flowing aerosols where individual particle sizing is not possible. In the SPSA, size is determined by the angular dependence of light scattering, as has been demonstrated by a number of workers using EPTs, for example, Davis et al. (1990). Our present technique of measuring the fluorescence cross section of a small number of particles yields accurate average cross sections, but simultaneous measurements of cross section and size requires measurements on a single suspended particle. Dry powder injection produces a cloud of particles from which it is difficult to pick out a single particle for analysis. Further refinement of fluorescence cross section measurements will require true single particle fluorescence measurements.

REFERENCES

Arakawa, E. T., Tumiiello, P. S., and Khare, B. N., Optical Properties of Horseradish Peroxidase and *Bacillus subtilis* Spores from 0.2 to 2.5 μm, US Army Research Office, Report number TCN 94346, 1995.

Arnold, S., and Folan, L. M., Fluorescence spectrometer for a single electrodynamically levitated microparticles, Rev. Sci. Instrum. 57, p. 2250, 1986.

Bronk, B. V., and Reinisch, L. Variability of Steady-State Bacterial Fluorescence with Respect to Growth Conditions, Spectrosc. 47 (4), p. 436, 1993.

Christesen, S., and Ong, K. Fluorescence Signatures of Biological Material, Presented at the MASINT Biological Defense Science and Technology Symposium, Patrick Air Force Base, Florida, 22-25 January, 1996.

Christesen, S. D., The U. S. Army Chemical and Biological Defense Command, ERDEC, Edgewood Proving Ground, MD, Personal Communication, 1997.

Davis, E. J., Buehler, M. F., and Ward, T. L., The Double-ring Electrodynamic Balance for Characterization, Rev. Sci. Inst., 61 (4), p.1281, 1990.

Faris, R. A., Copeland, D. J., Eckstrom, A., Williams, C., Witham, C., Carlisle, C. B., Leonelli, J., and Bronk, B., Spectrally Resolved Absolute Fluorescence Cross Sections of B. globigii and B. Cereus, SRIN Technical Note, Project # 2913, Contract # DAAA15-91-D-0002, May, 1992.

Fung, K. H., and Tang, I. N., Composition Analysis of Suspended Aerosol Particles by Raman Spectroscopy: Sulfates and Nitrates, J. Colloid and Interface Sci. 130 (1), p.219, 1989.

Gouesbet, G., and Grehan, G., (Eds.), Optical Particle Sizing, Theory and Practice, Plenum Press, New York, NY, 1991.

Grader, G. S., and Arnold, S., Fourier Transform Infrared Spectroscopy of a Single Aerosol Particle, J. Chem. Phys., 86 (11), p. 5897, 1987.

Mulholland, G. W., Hartman, A. W., Hembree, G. G., Marx, E., and Lettieri, T. R., Development of a one-micron-diameter particle size standard reference material, J. Res. National Bureau of Standards, 90, p. 3, 1985.

Ong, K. and S. D. Christesen, Fluorescence Signatures of Biological Material, in: Proceedings of the 1996 Edgewood ERDEC Scientific Conference on Obscuration and Aerosol Research, Aberdeen Proving Ground, MD, June 7-9, 1996

Paul, W., and Raether, M., Das elektrische massenfilter, A. Phys. 140, p. 262, 1955.

Stephens, J. R. and Rubel, G., Studies of Fluorescence Spectra and Effect of Humidity of Bioaerosols, presented at the MASINT Biological Defense Science and Technology Symposium, Jan 23-25, Patrick AFB, Florida, 1996.

Stephens, J. R., Fluorescence Cross Section Measurements of Biological Agent Simulants, in: Proceedings of the Scientific Conference on Obscuration and Aerosol Research, June 25-28, 1996, Aberdeen, Maryland, (in press), 1996a.

Stephens, J. R., Measurements of Fluorescence Cross Sections of Biological Agent Simulants, in: Proceedings of the Conference on Chemical and Biological Defense Research, Aberdeen Proving Ground, MD, November 19-22, 1996b.

Taflin, D. C., and Davis, E. J., A study of aerosol chemical reactions by optical resonance spectroscopy, J. Aerosol Sci., 21, p. 73, 1990.

Taflin, D. C., Ward, T. L., and Davis, E. J., Electrified droplets fission and the Raleigh limit, Langmuir, 5, p. 376, 1989.

Whitten, W. B., Ramsey, Arnold, S., Bronk, B. V., Single molecule detection limits in levitated microparticles, Anal. Chem., 63, p. 1027, 1991.

Wuerker, R. F., Shelton, H., and Langmuir, R. V., Electrodynamic containment of charged particles, J. Appl. Phys., 30, p. 342, 1959.

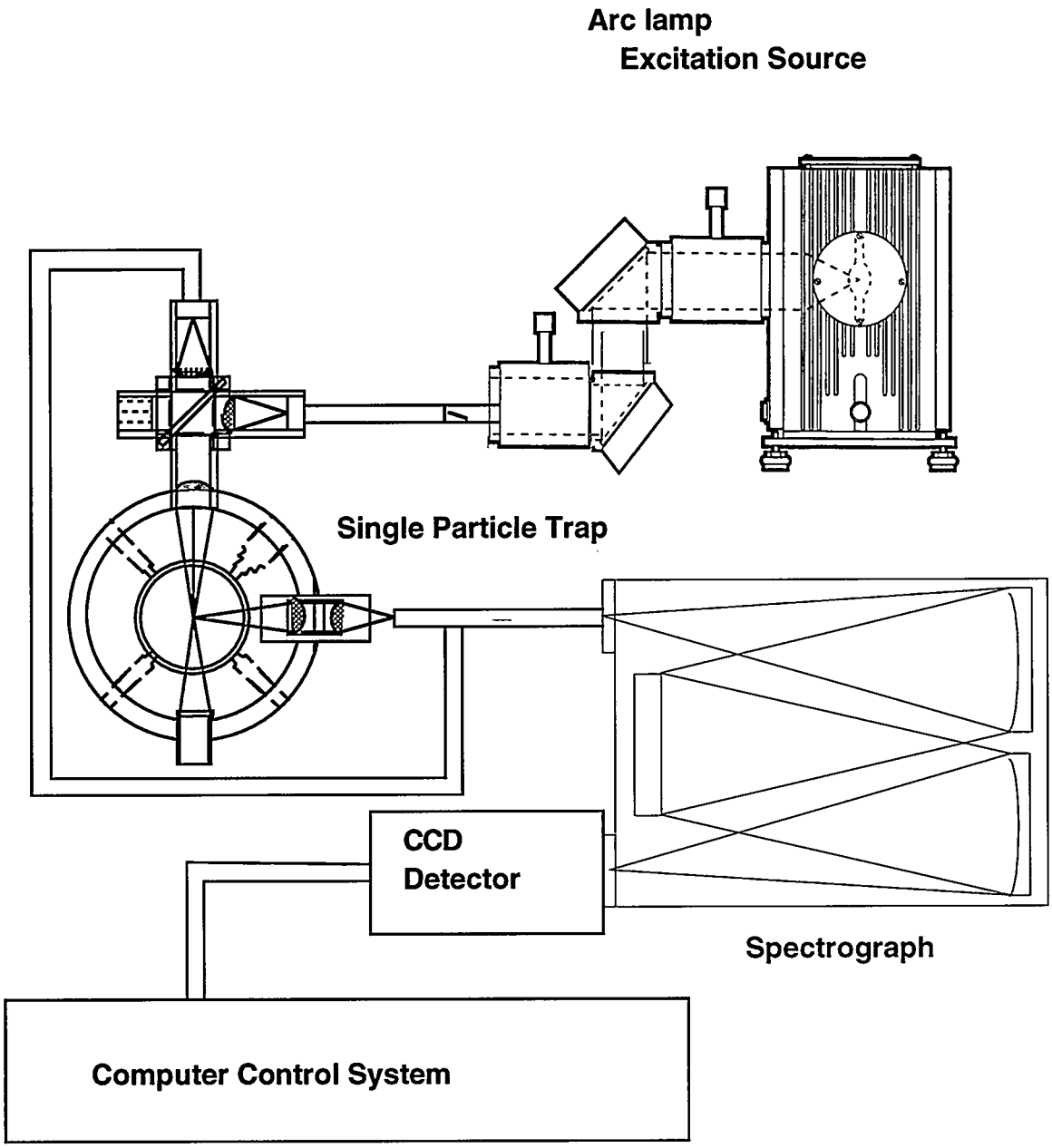

Figure 1. Schematic of the Single Particle Spectroscopy Apparatus (SPSA)

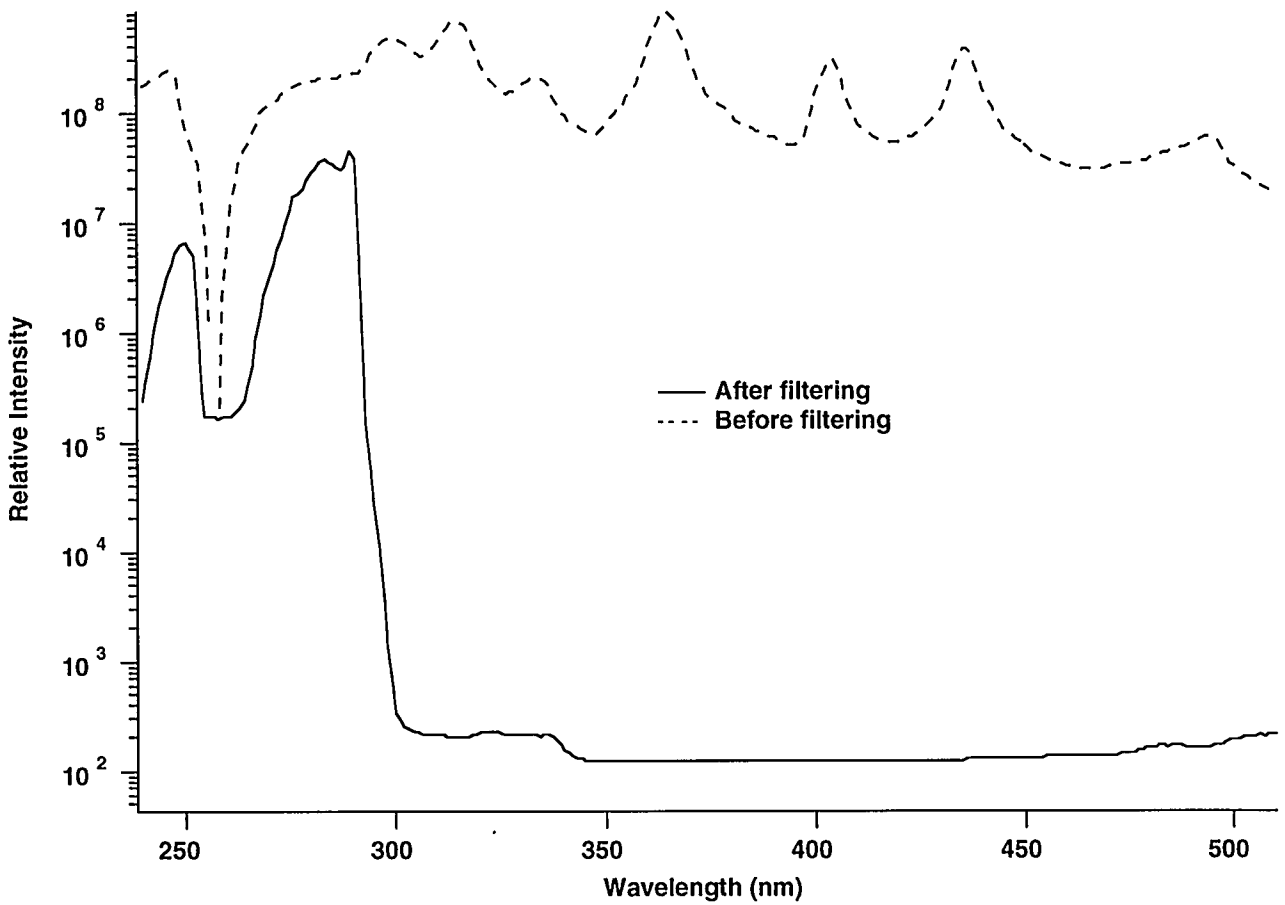

Figure 2. Output of Hg lamp before and after optical filtering

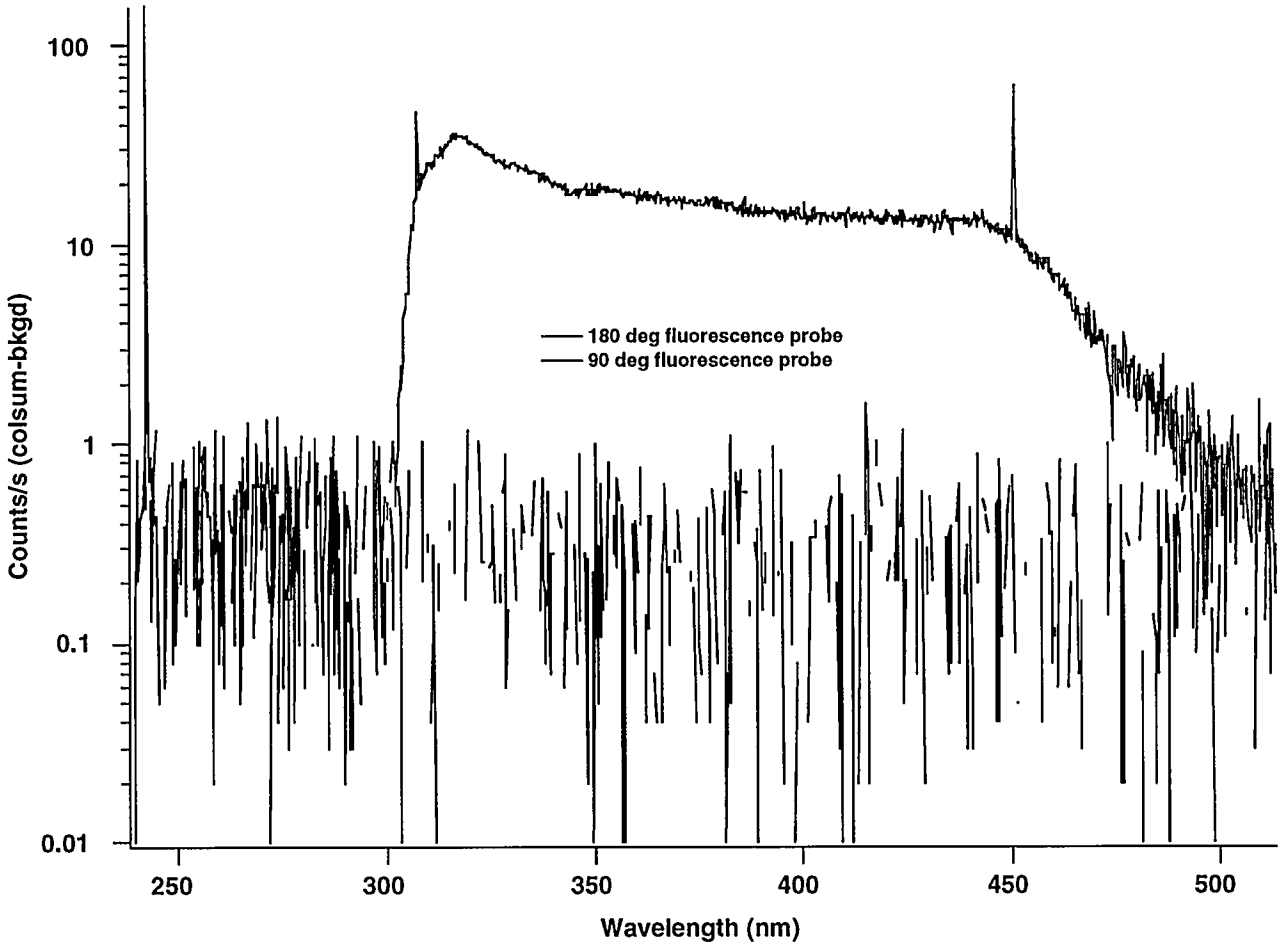

Figure 3. Measured background scattered light from particle at 90 and 180 degrees collection angle

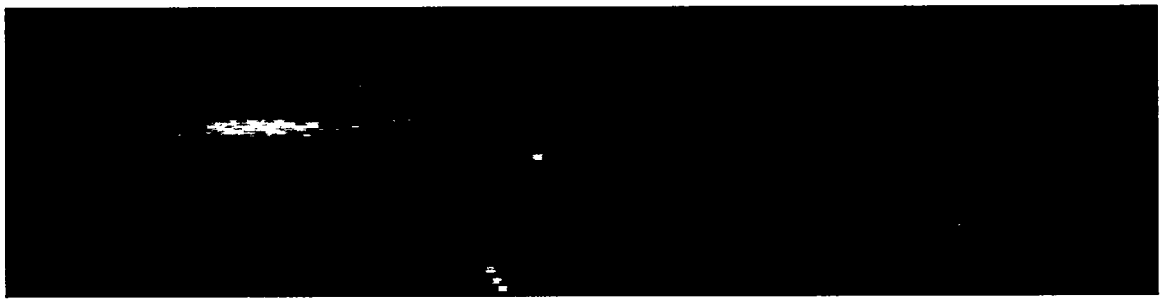

Figure 4. CCD image of B. megaterium spectrum (290 - 450 nm)

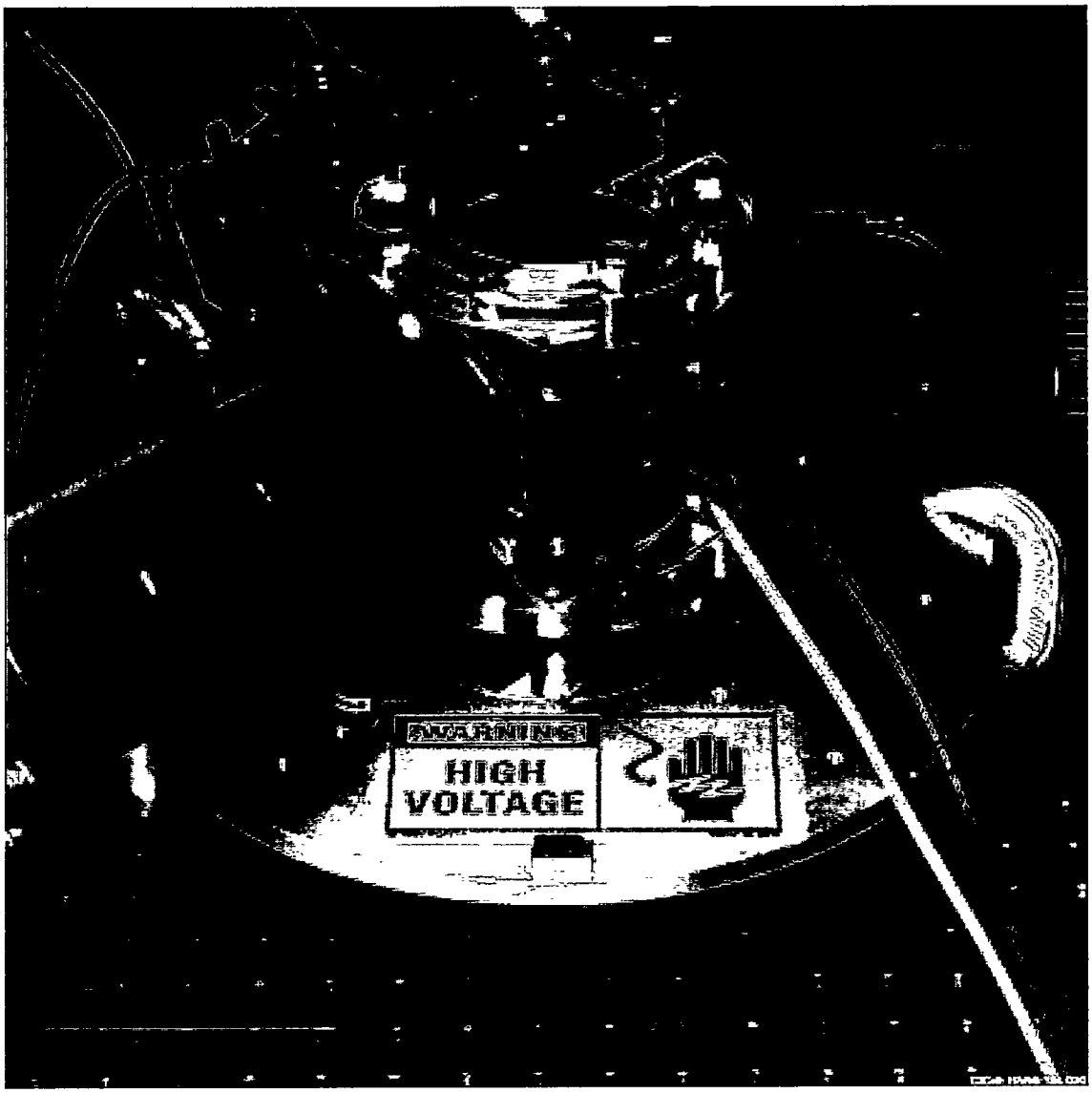

Figure 5. Close-up of the Single Particle Spectroscopy Apparatus

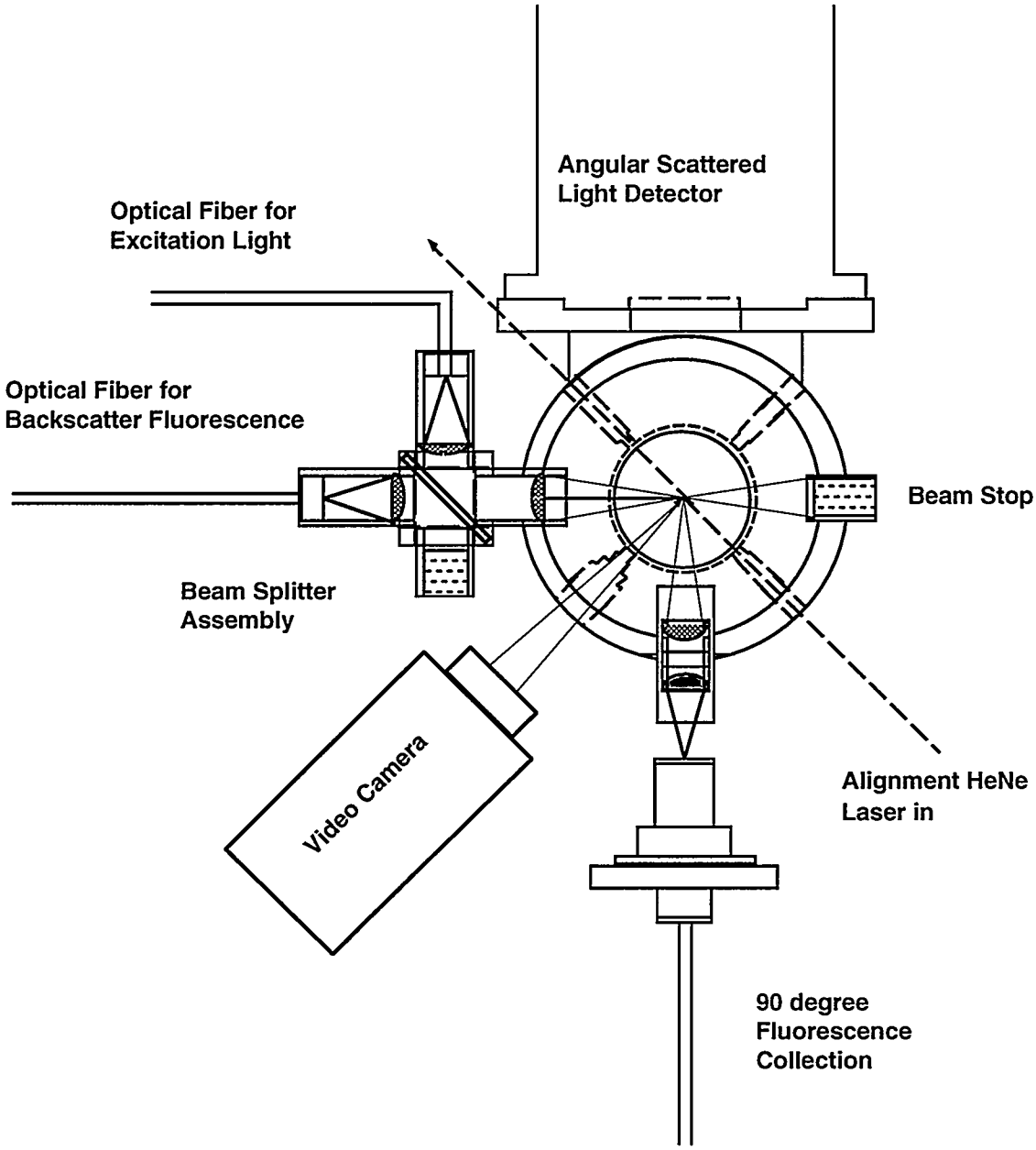

Figure 6. Detail Schematic of the Single Particle Spectroscopy Apparatus

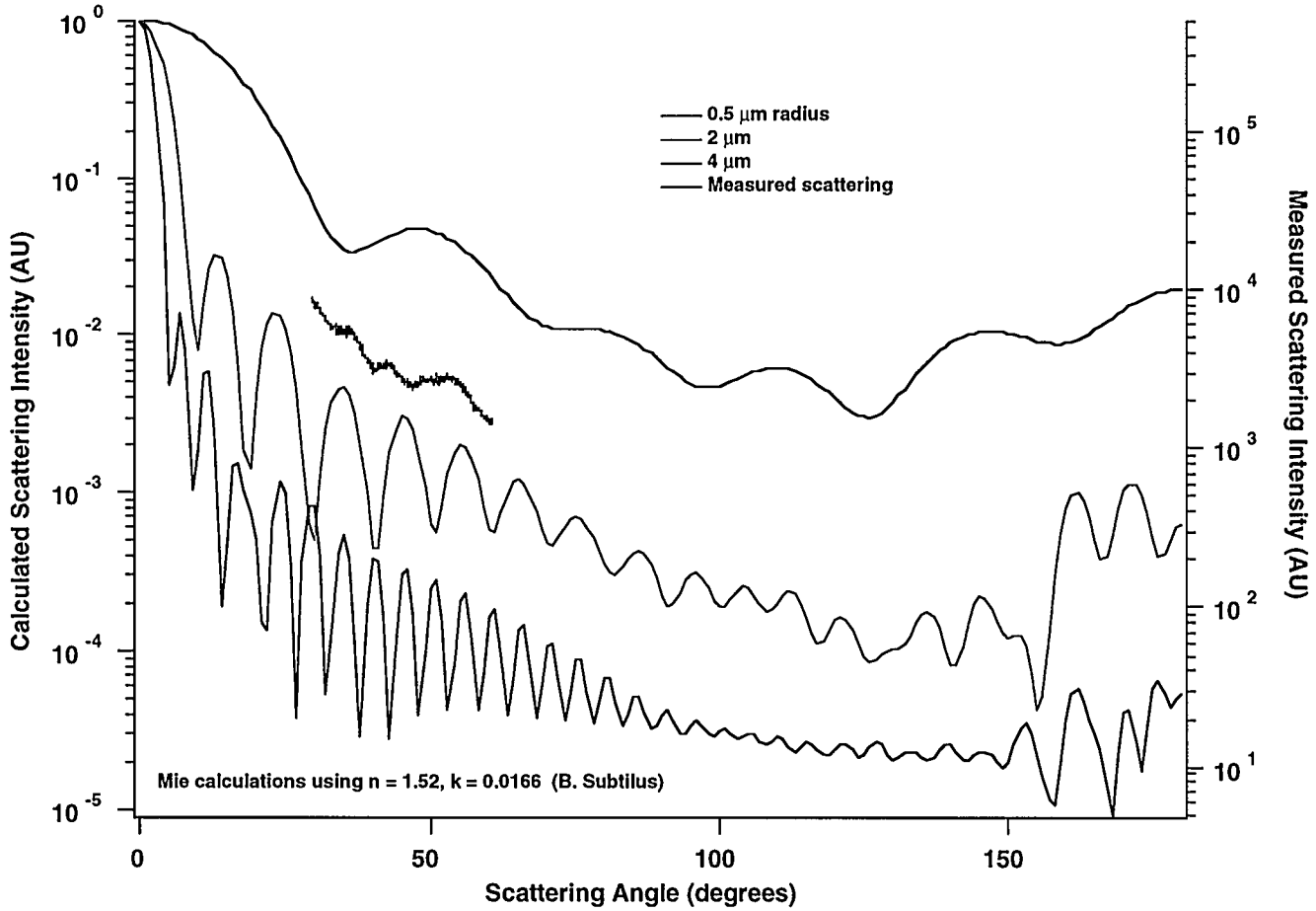

Figure 7. Calculated *B. subtilis* and measured *B. megaterium* scattering versus angle for particle sizing

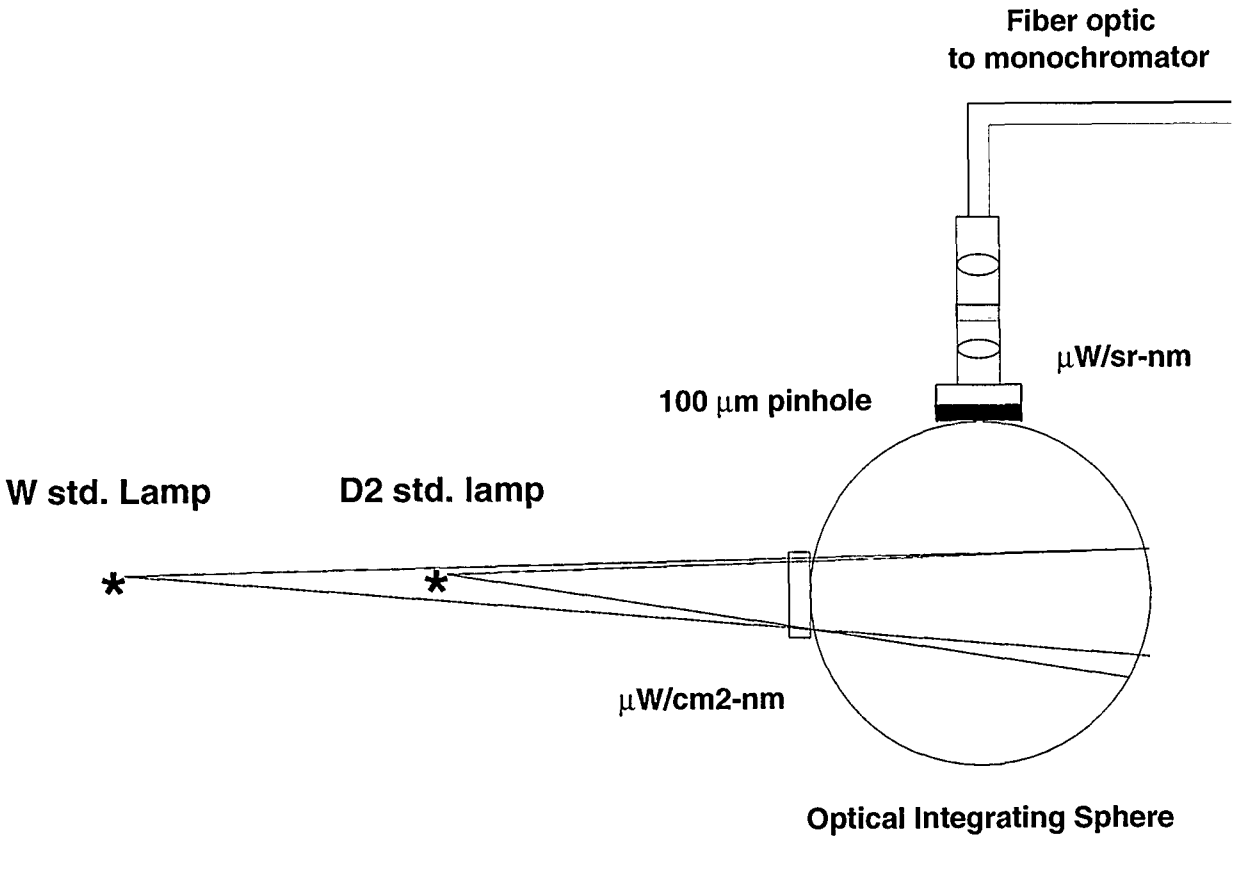

Figure 8. Calibration of exciation and fluorescence optics

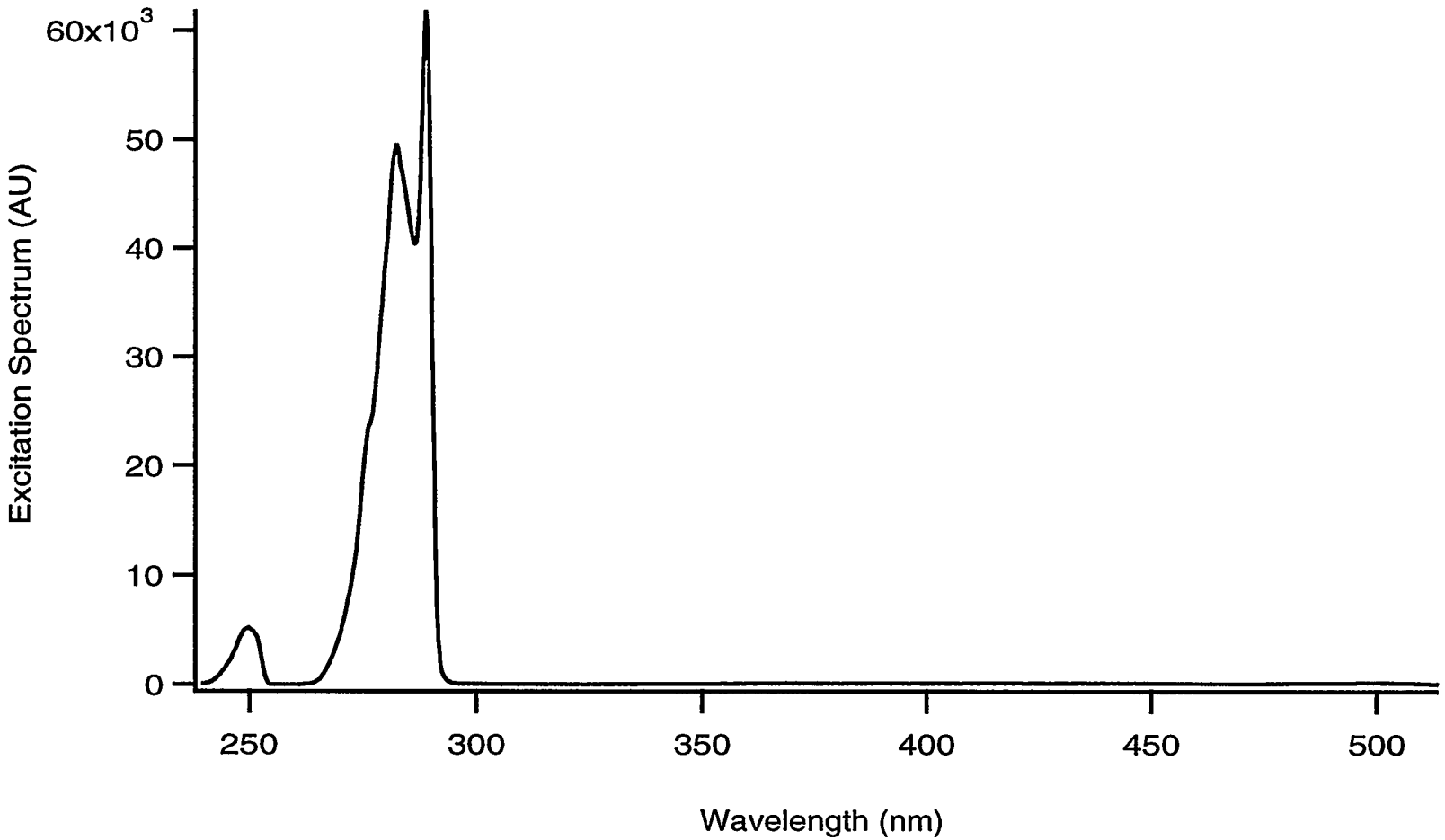

Figure 9. Excitation spectrum of filtered arc lamp

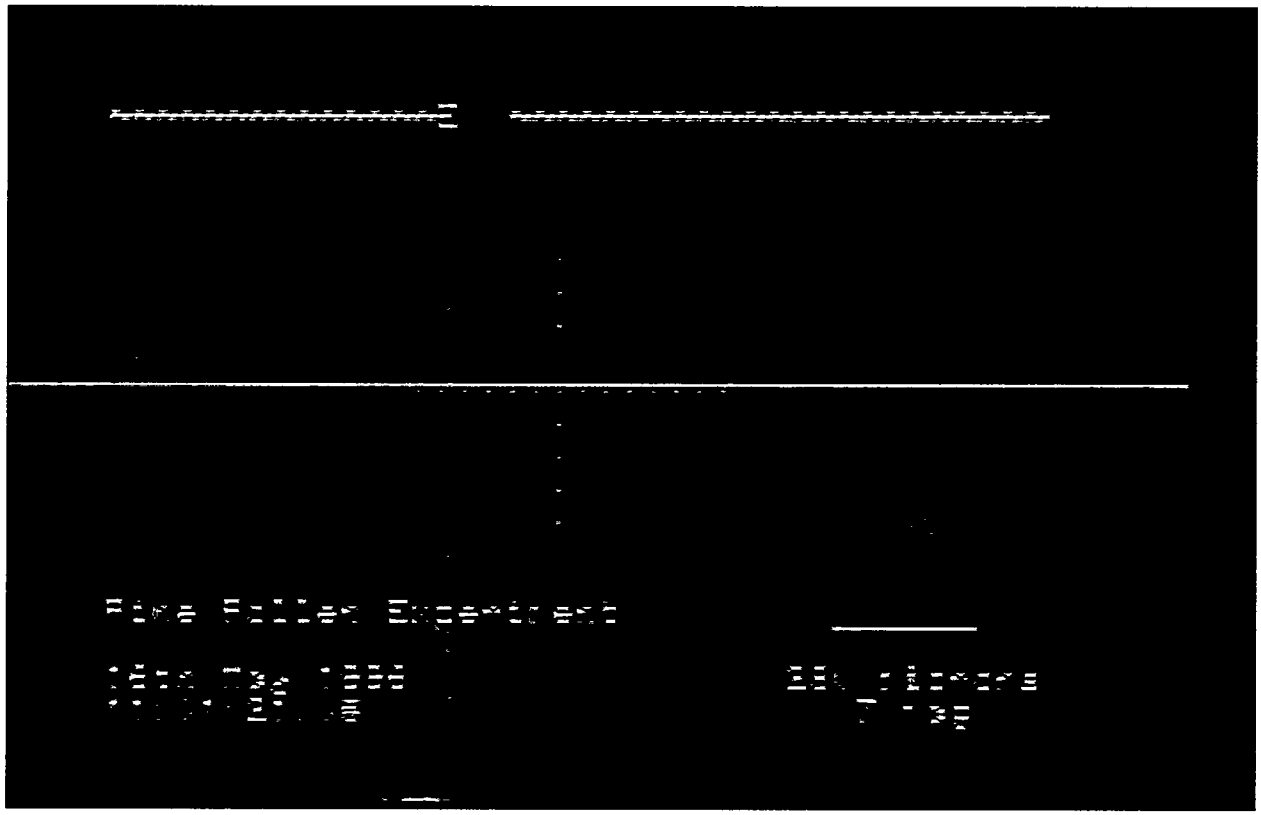

Figure 10. Measurement of excitation fiber focus

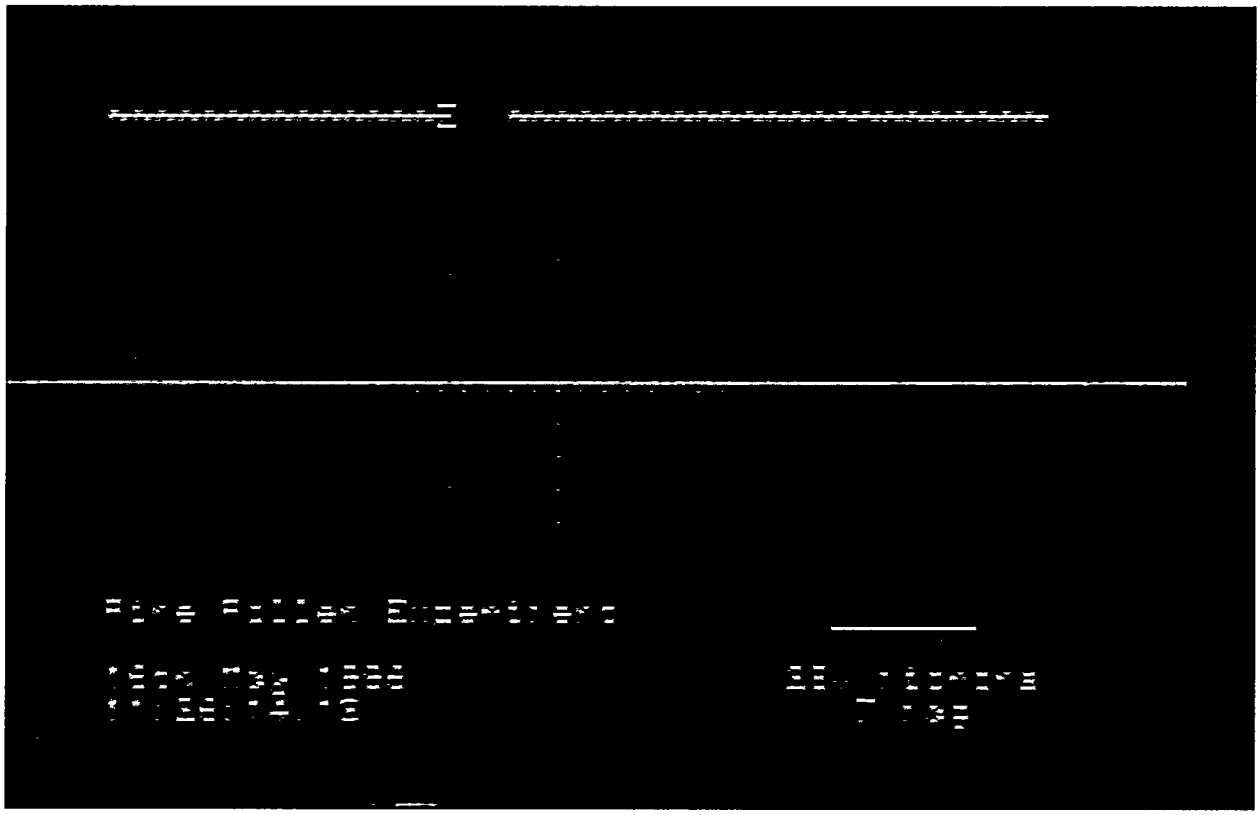

Figure 11. Measurement of fluorescence fiber focus

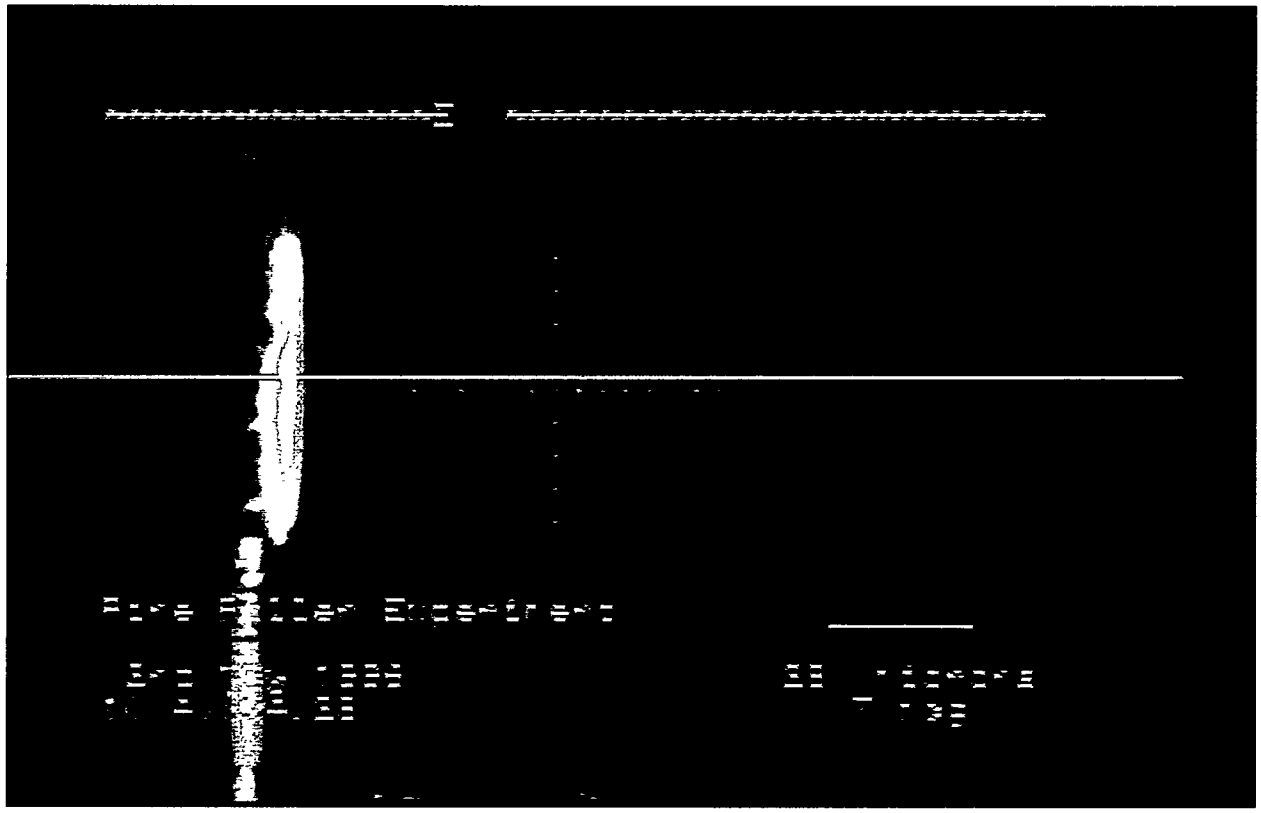

Figure 12. Alignment of exciation light on scintillation fiber

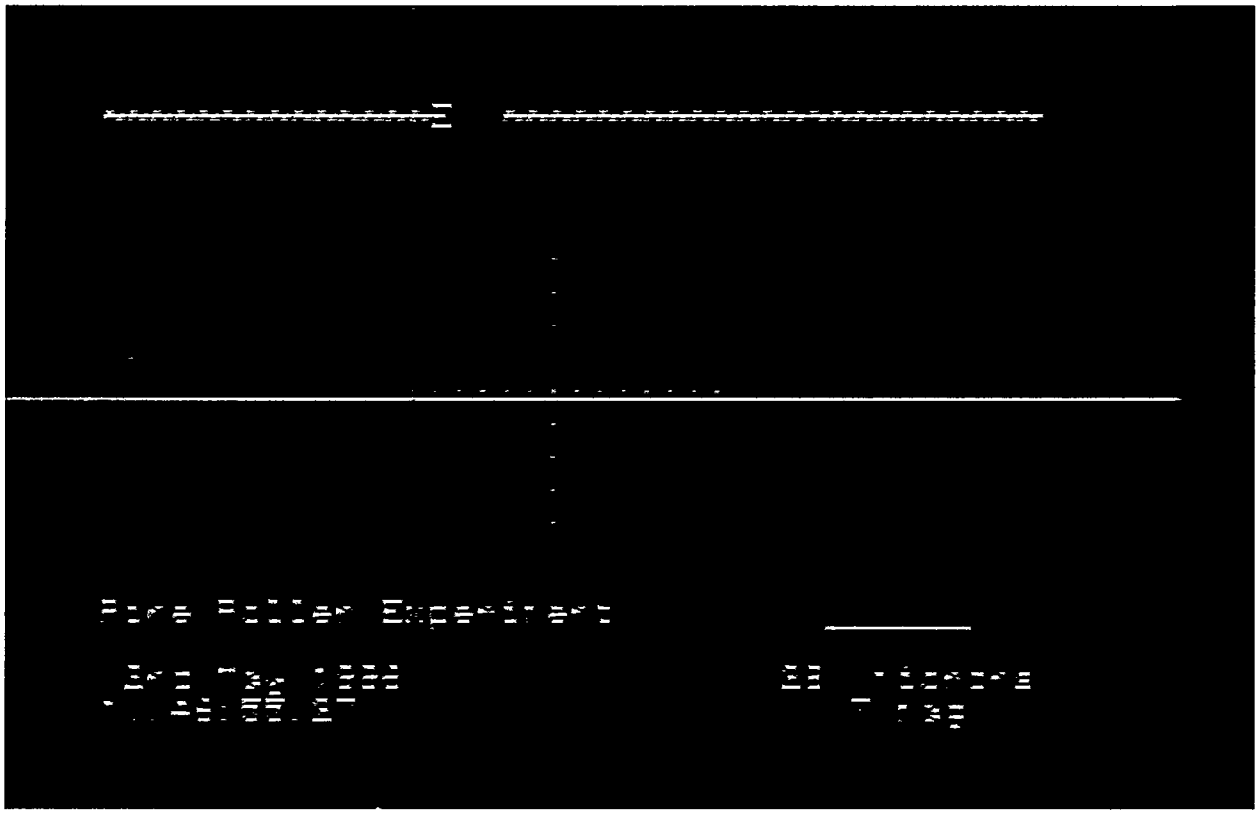

Figure 13. Alignment of fluorescence probe on scintillation fiber

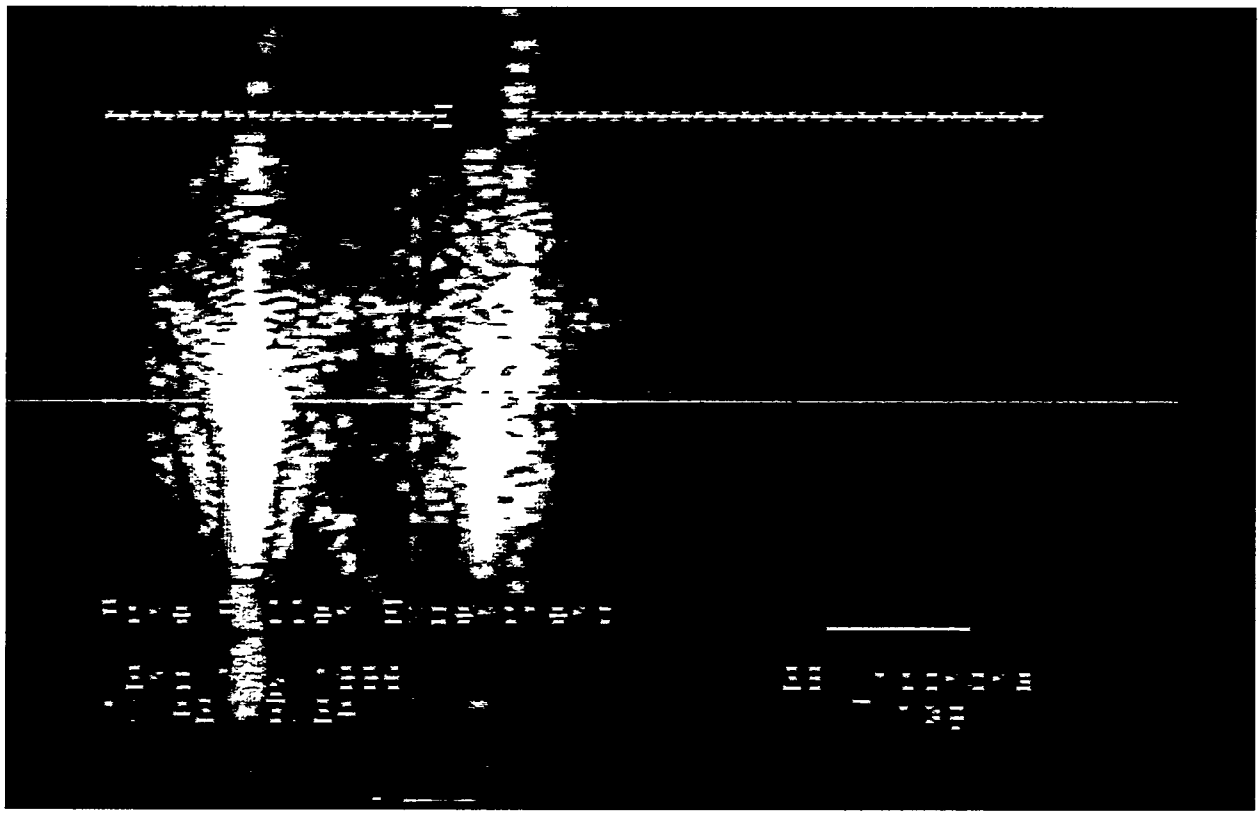

Figure 14. Alignment of HeNe laser on scintillation fiber

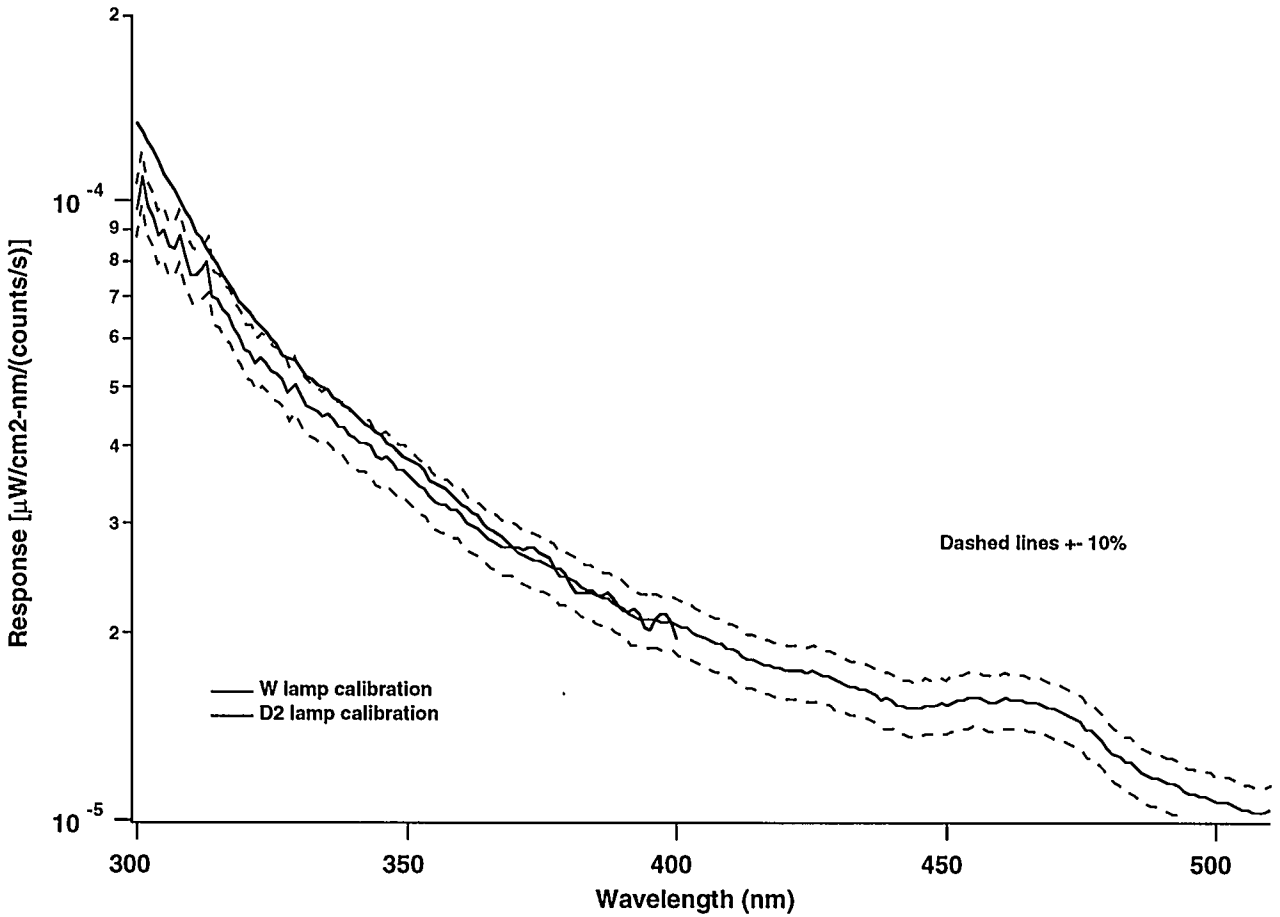

Figure 15. Calibration of fluorescence optics with standard lamps

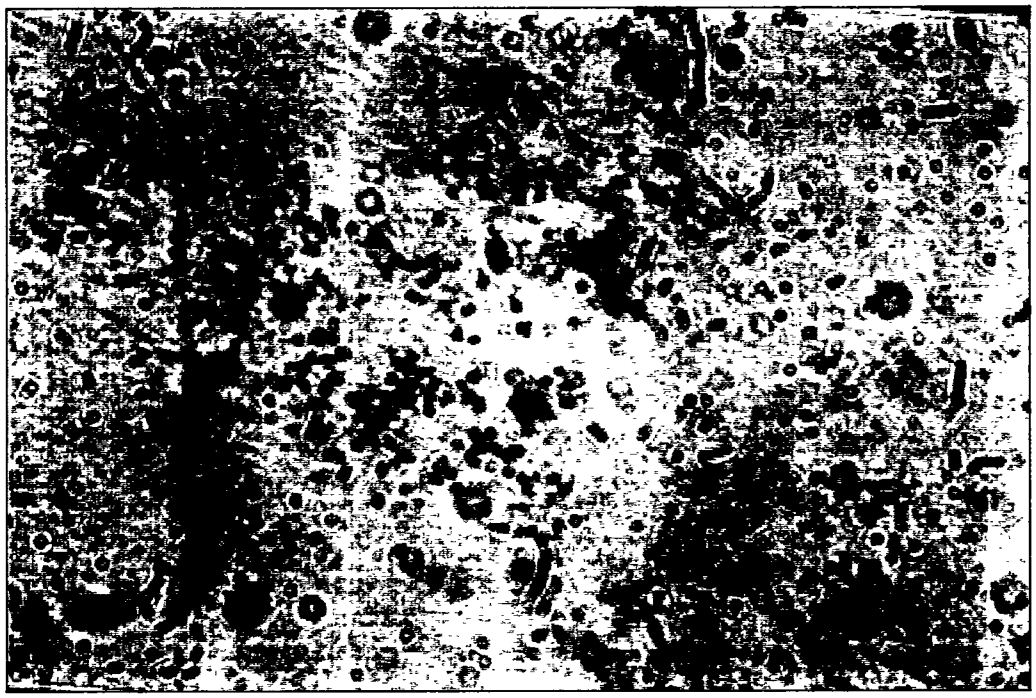

Figure 16. Optical Micrograph of *Bacillus globigii* from CBDCOM

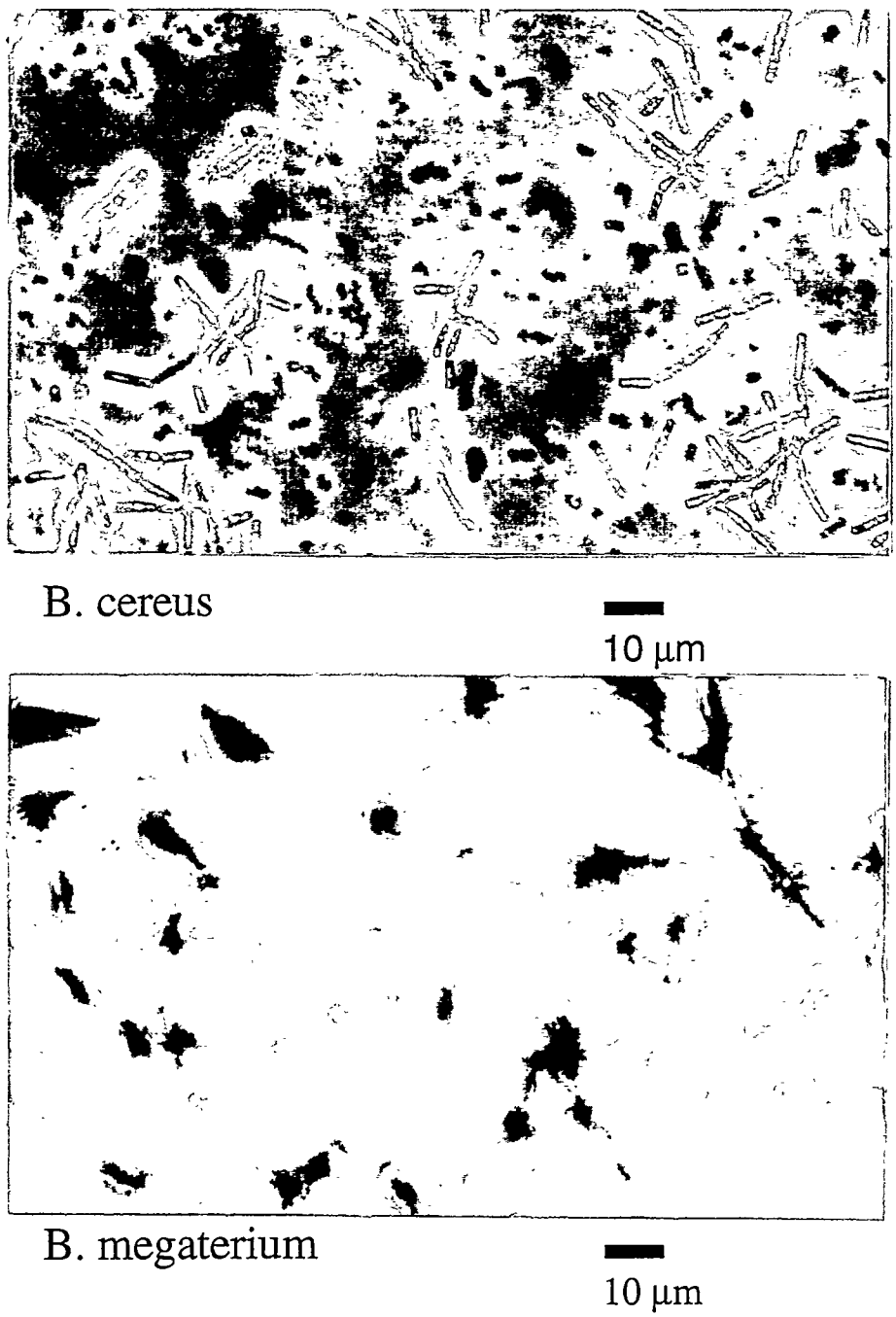

Figure 17. Optical micrographs of Los Alamos grown *B. anthracis* simulants

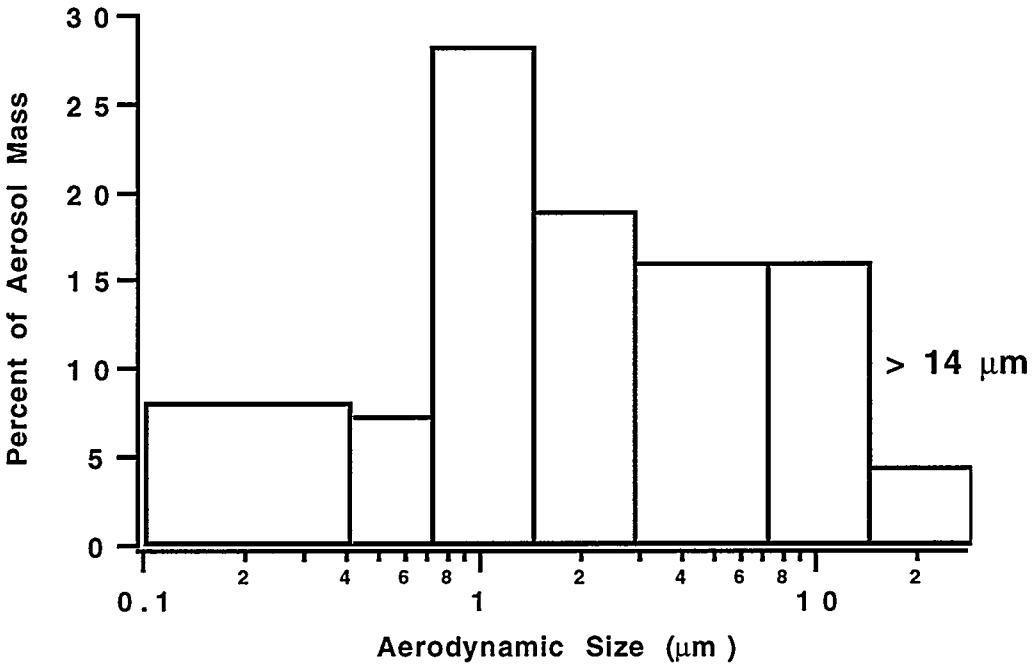

(A) Before spore separation

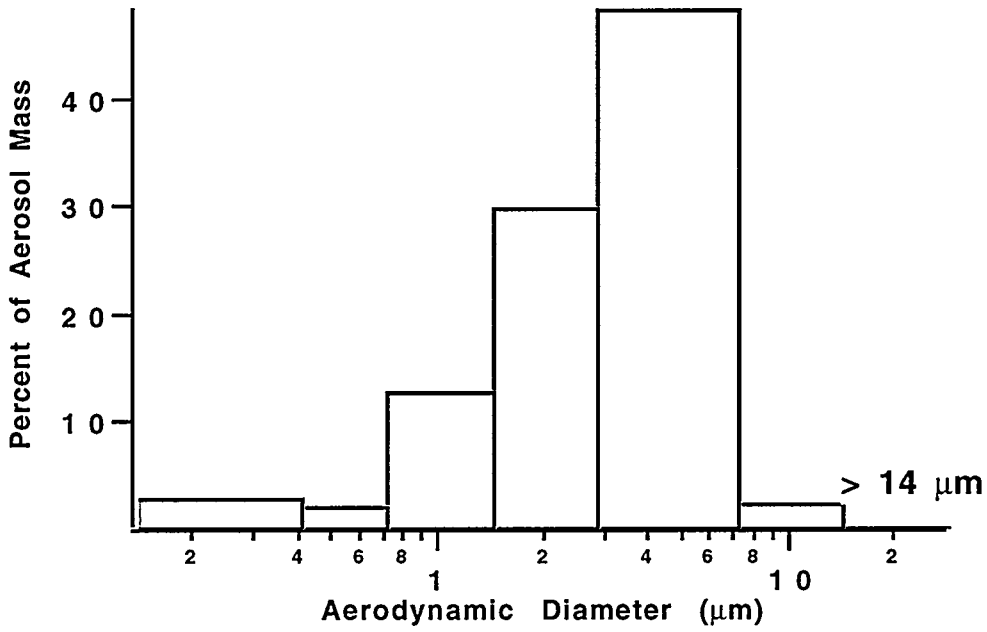

(B) After spore separation

Figure 18. Size distributions of *B. subtilis* before and after spore separation

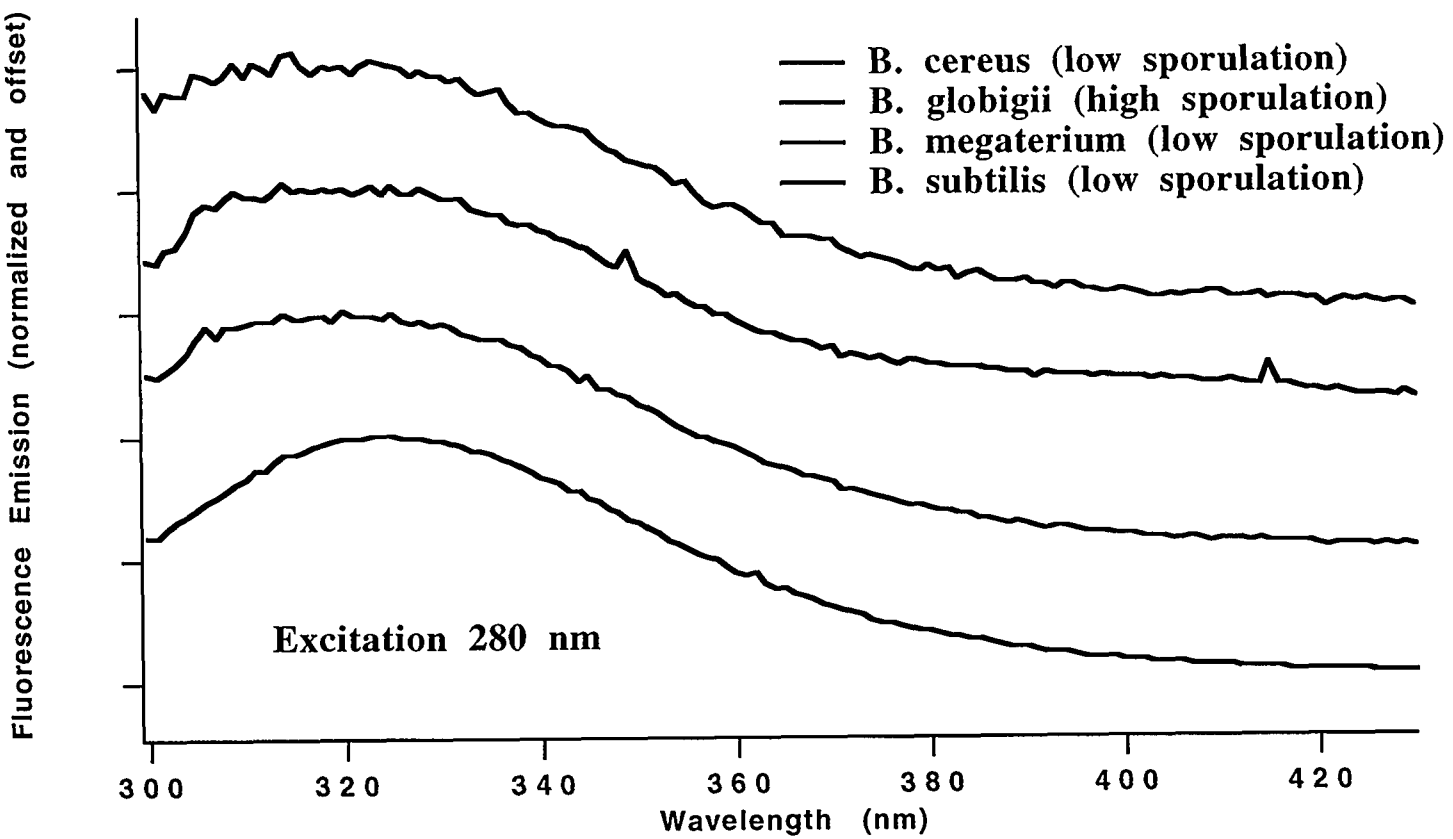

Figure 19. Fluorescence spectra of *B. anthracis* simulants suspended in water

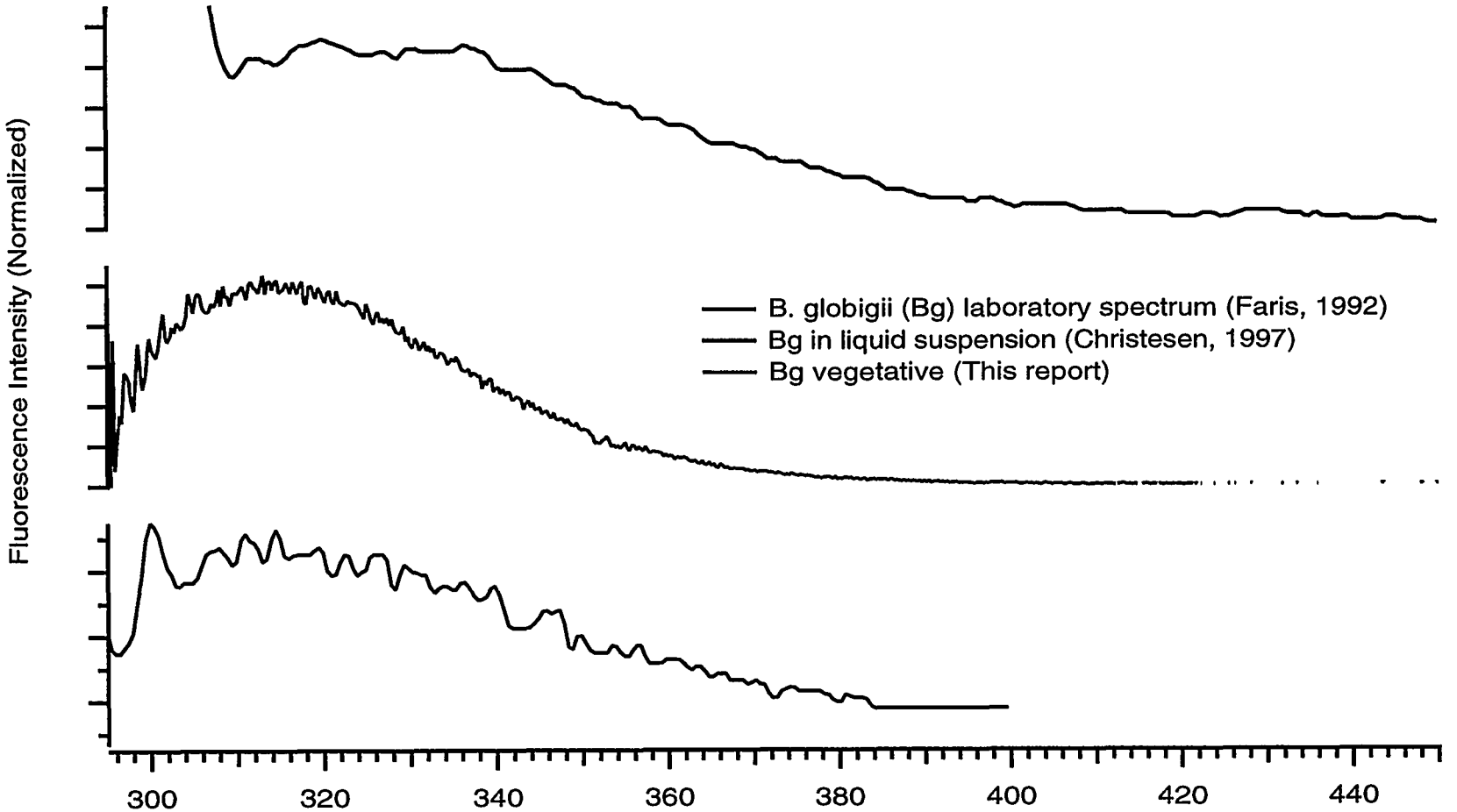

Figure 20. Comparison of fluorescence from this work and literature spectra

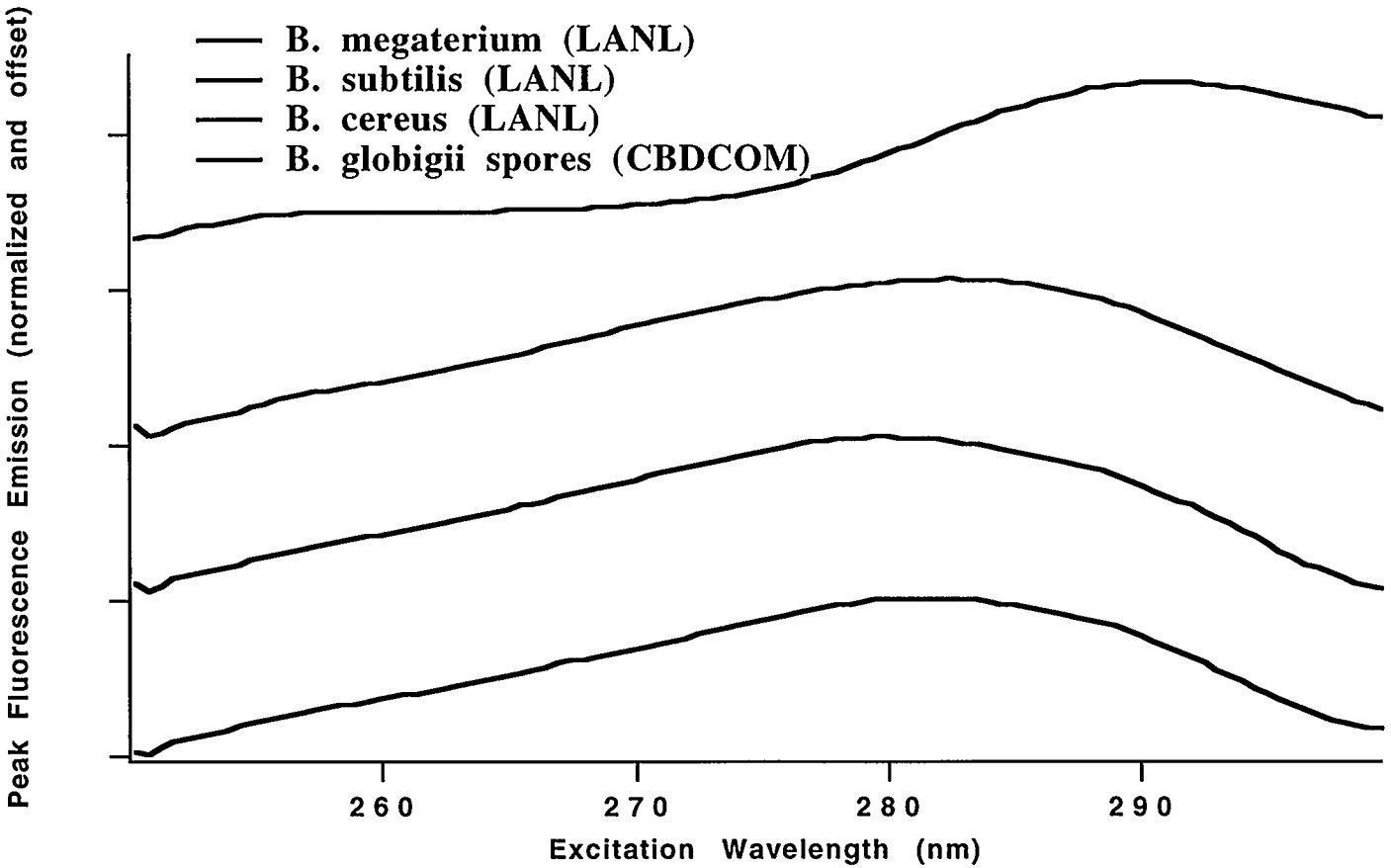

Figure 21. Excitation spectra of *B. anthracis* simulants suspended in water (fluorescence at 350 nm)

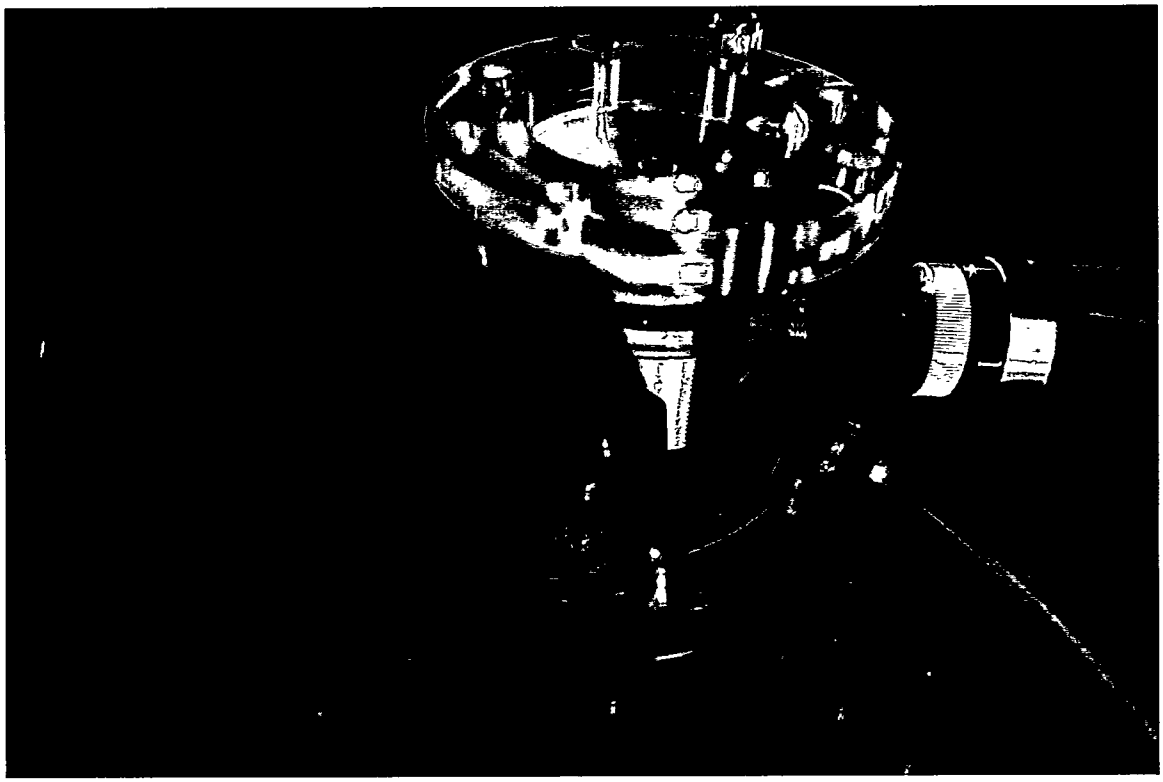

Figure 22 Fluorescent microsphere suspended in the Single Particle Spectroscopy Apparatus

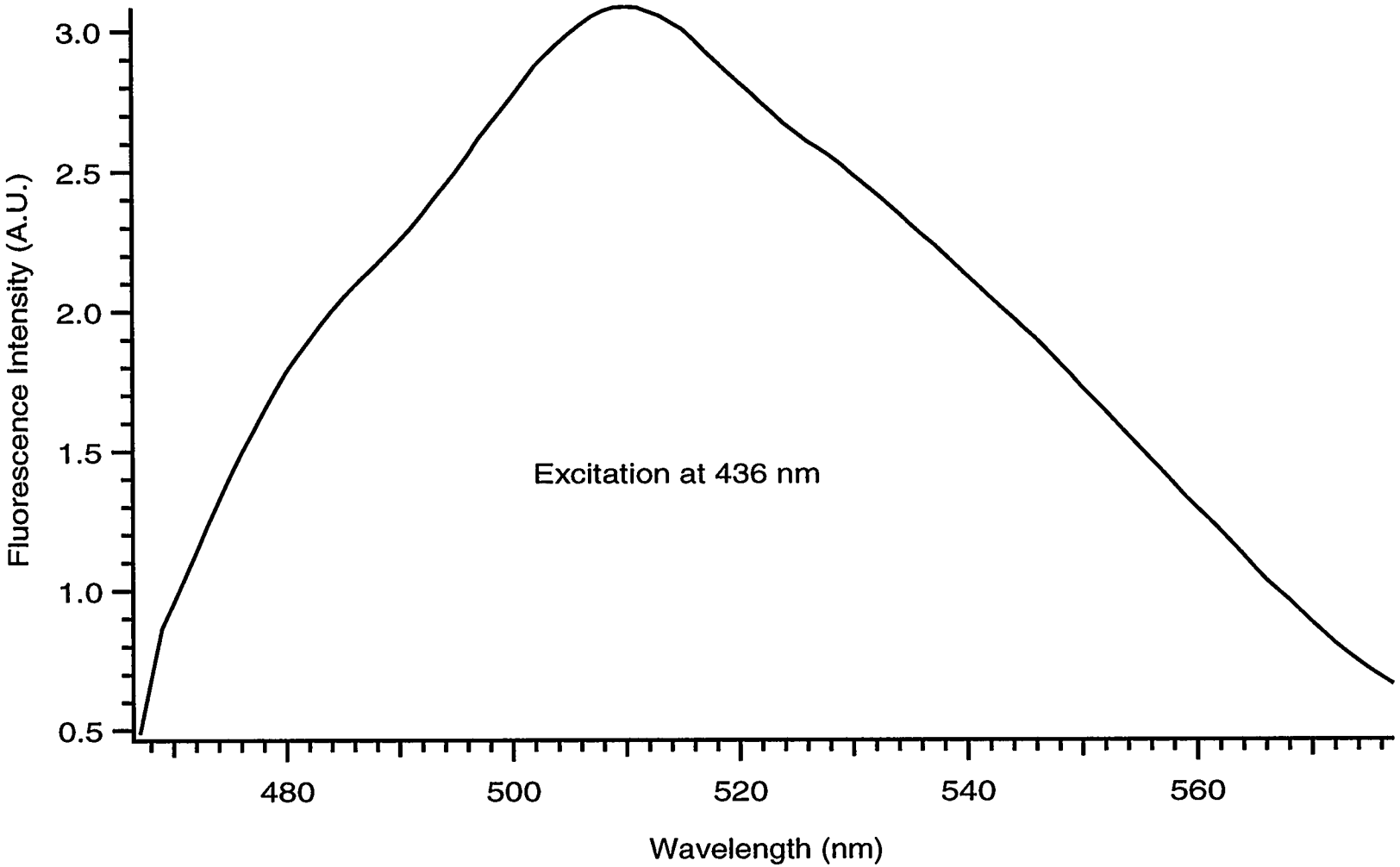

Figure 23 Fluorescence spectrum of suspended fluorescent microsphere

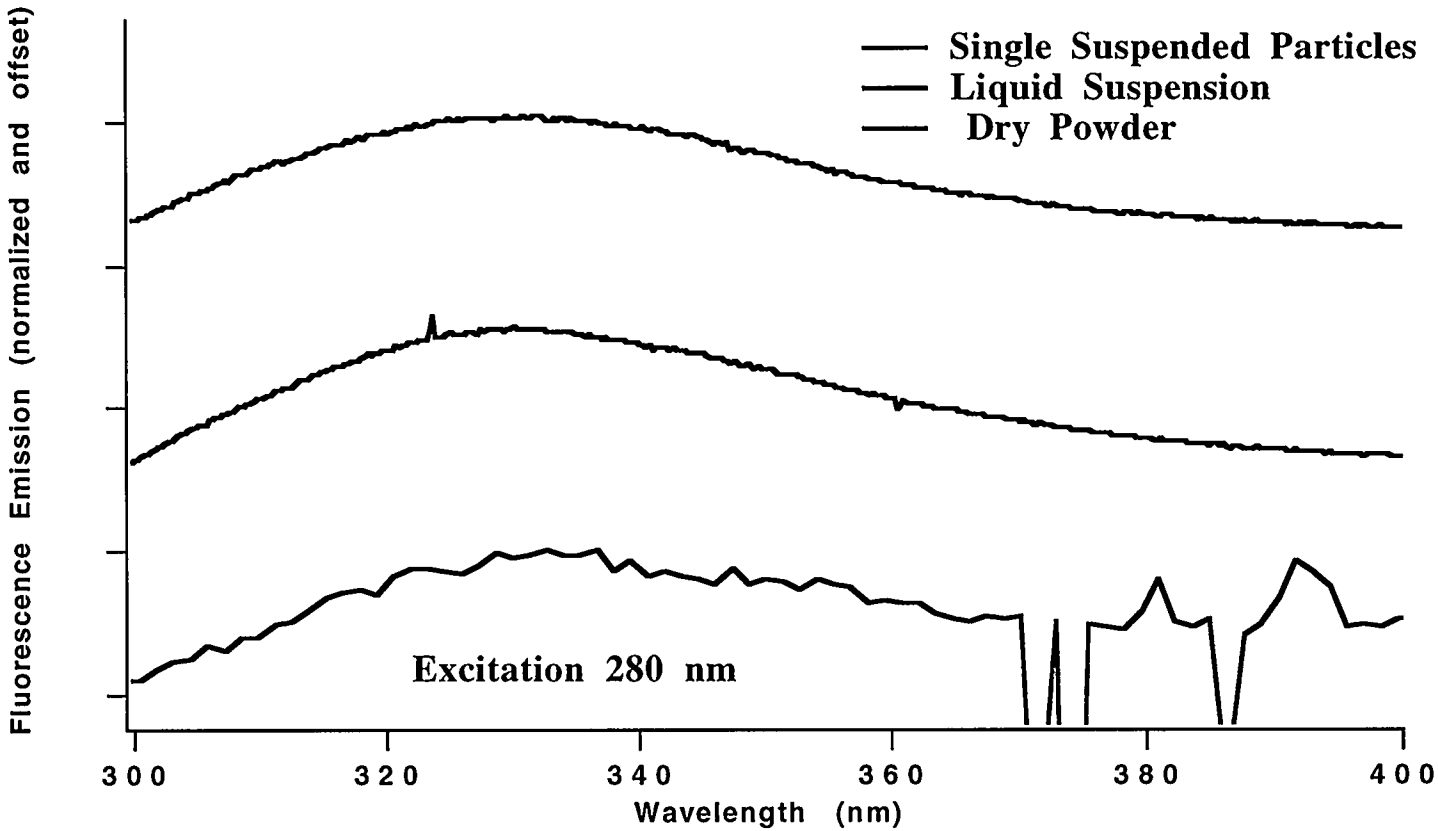

Figure 24 Comparison of fluorescence spectra from *B. cereus* versus preparation method

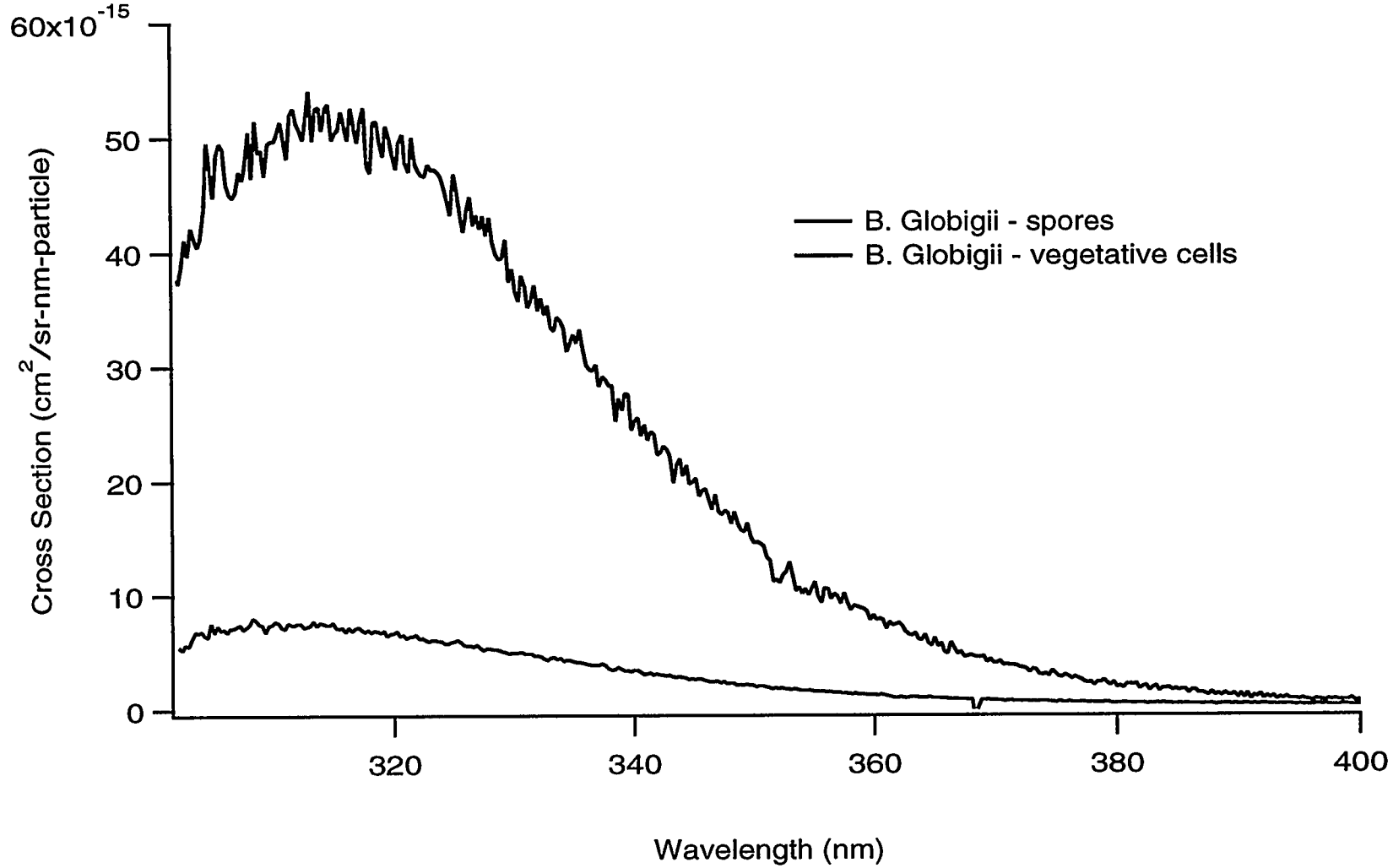

Figure 25 Fluorescence cross sections of *B. globigii* spores and vegetative cells

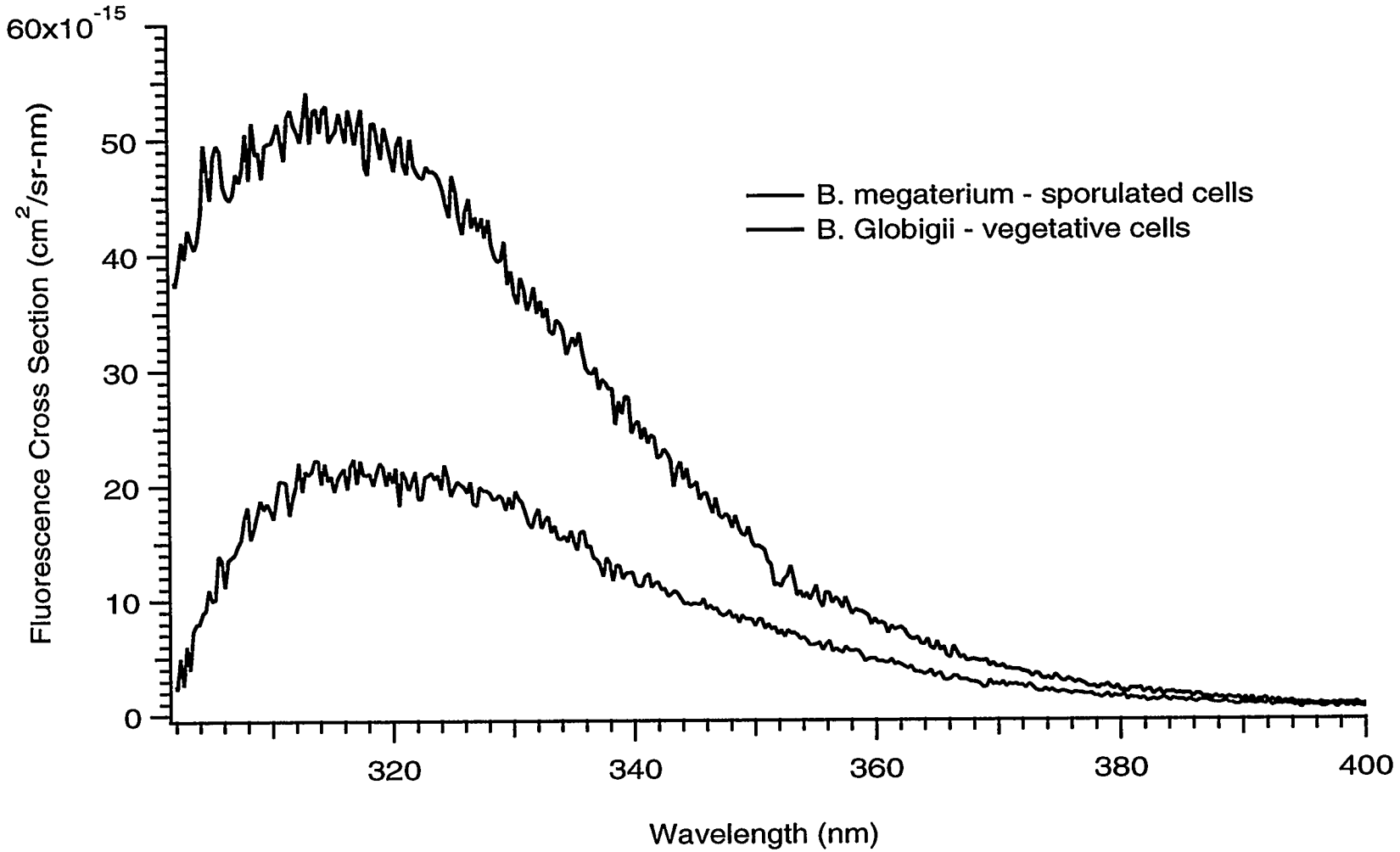

Figure 26 Fluorescence cross sections of *B.globigii* and *B. megaterium* cells

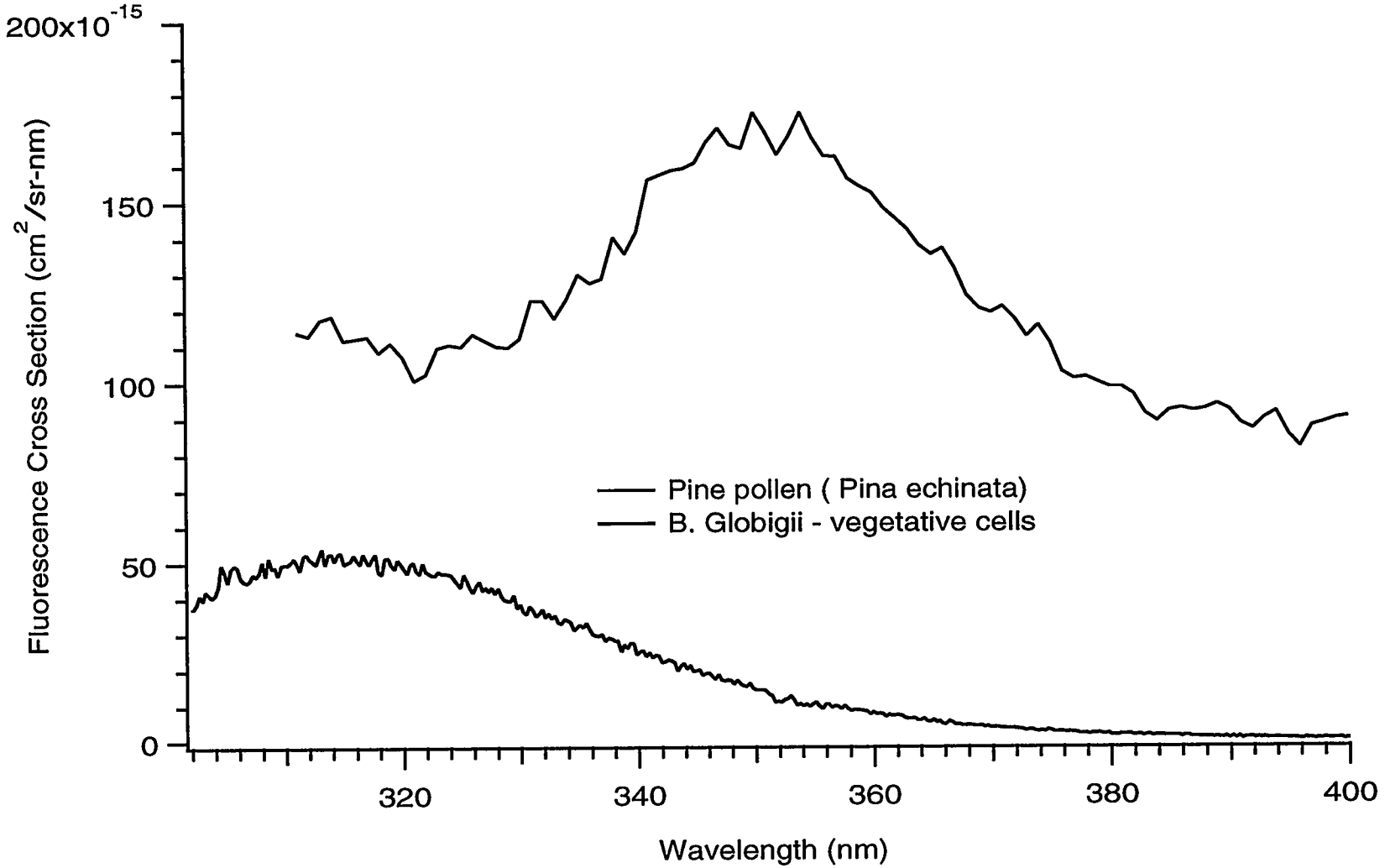

Figure 27 Fluorescence cross sections of *B.globigii* cells and pine pollen particles